

## Supporting Information

### **Diaqua- $\beta$ -Octaferrocenyltetraphenylporphyrin: A Multiredox-active and Air-stable $16\pi$ Non-Aromat**

Rasha K. Al-Shewiki,<sup>†</sup> Marcus Korb,<sup>†</sup> Alexander Hildebrandt,<sup>†</sup> Stefan Zahn,<sup>‡</sup> Sergej Naumov,<sup>‡</sup> Roy Buschbeck,<sup>†</sup> Tobias Rüffer,<sup>\*†</sup> and Heinrich Lang<sup>†</sup>

<sup>†</sup>Inorganic Chemistry Department, Chemnitz University of Technology, Strasse der Nationen 62, Chemnitz 09107, Germany.

<sup>‡</sup>Chemical Department, Leibniz Institute of Surface Modification (IOM), Permoserstrasse 15, 04318 Leipzig, Germany.

E-mail: tobias.rueffer@chemie.tu-chemnitz.de

## Table of Contents

1.	Experimental Details.....	S3
1.1	General Information.....	S3
1.2	Synthesis and Analytical Data of <b>H<sub>2</sub>TPP</b> and <b>CuTPP</b> .....	S3-S4
1.3	Synthesis and Analytical Data of <b>CuTPPBr<sub>8</sub>·CHCl<sub>3</sub></b> and <b>{TPPFc<sub>8</sub>(H<sub>2</sub>O)<sub>2</sub>}</b> .....	S5-S6
1.4	Purification of <b>CuTPPBr<sub>8</sub>·CHCl<sub>3</sub></b> and <b>{TPPFc<sub>8</sub>(H<sub>2</sub>O)<sub>2</sub>}</b> .....	S7
1.4.1	Comments to the synthesis and isolation of <b>{TPPFc<sub>8</sub>(H<sub>2</sub>O)<sub>2</sub>}</b> .....	S8-S9
1.5	<sup>1</sup> H and <sup>13</sup> C NMR spectra of <b>H<sub>2</sub>TPP</b> .....	S10
1.6	HR-ESI-TOF-MS and IR spectra of <b>H<sub>2</sub>TPP</b> .....	S11
1.7	HR-ESI-TOF-MS and IR spectra of <b>CuTPP</b> .....	S12
1.8	HR-ESI-TOF-MS and IR spectra of <b>CuTPPBr<sub>8</sub>·CHCl<sub>3</sub></b> .....	S13
1.9	HR-ESI-TOF-MS and IR spectra of <b>{TPPFc<sub>8</sub>(H<sub>2</sub>O)<sub>2</sub>}</b> .....	S14
2.	UV-vis absorption spectra.....	S15
2.1	Concentration dependent UV-vis spectra and data of <b>H<sub>2</sub>TPP</b> .....	S15
2.2	Concentration dependent UV-vis spectra and data of <b>CuTPP</b> .....	S16
2.3	Concentration dependent UV-vis spectra and data of <b>CuTPPBr<sub>8</sub>·CHCl<sub>3</sub></b> .....	S17
2.4	Concentration dependent UV-vis spectra and data of <b>{TPPFc<sub>8</sub>(H<sub>2</sub>O)<sub>2</sub>}</b> .....	S18
3.	Electrochemical Measurements.....	S19-S21
4.	Selected antiaromatic 16π tetraphenylporphyrins.....	S22
5.	Crystallography.....	S22
5.1	Experimental Details.....	S22-S23
5.2	Structural Data of <b>CuTPPBr<sub>8</sub>·2CH<sub>2</sub>Cl<sub>2</sub></b> and <b>{TPPFc<sub>8</sub>(H<sub>2</sub>O)<sub>2</sub>}</b> ·5CH <sub>2</sub> Cl <sub>2</sub> .....	S23-S28
5.3	$\beta$ -2,3,7,8,12,13,17,18-Octabromo-meso-5,10,15,20-tetraphenyl(metallo) porphyrins ( <b>H<sub>2</sub>TArylBr<sub>8</sub></b> / <b>MTArylBr<sub>8</sub></b> ).....	S29-S32
6.	Computational Details.....	S32
7.	References.....	S32-S34

## Experimental Details

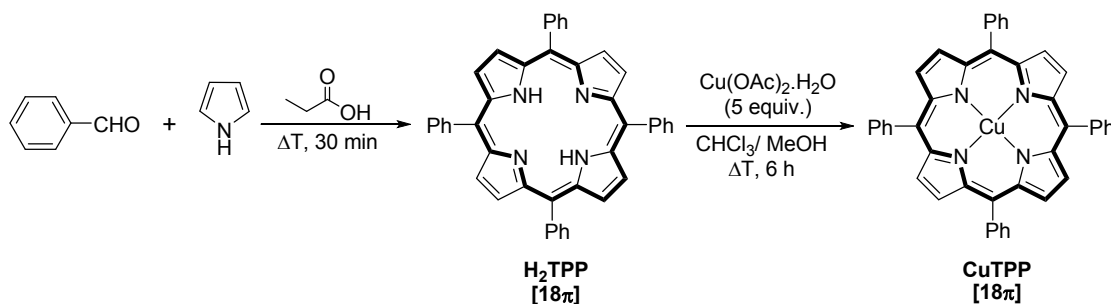
### 1.1 General Information

The Negishi *C,C* cross-coupling reactions were carried out under an atmosphere of argon using standard Schlenk techniques. Tetrahydrofuran (THF) was purified before use by distillation from sodium/benzophenone ketyl,<sup>1</sup> while, dichloromethane (CH<sub>2</sub>Cl<sub>2</sub>) was dried with an MBraun MB SPS-800 system (double column solvent filtration, working pressure 0.5 bar) and further purified by distillation from calcium hydride.<sup>1</sup>

<sup>1</sup>H and <sup>13</sup>C NMR spectra were recorded at ambient temperature with a Bruker Avance III 500 Ultra Shield Spectrometer in the Fourier transform mode. The spectra were recorded at 500.300 MHz (<sup>1</sup>H) and 125.813 MHz (<sup>13</sup>C), respectively. The chemical shifts (δ) are given in parts per million (ppm), and for referencing, the solvent signals were used (CDCl<sub>3</sub>: 7.26 ppm (<sup>1</sup>H), 77.16 ppm (<sup>13</sup>C)). Fourier transform infrared spectroscopy (FTIR) studies in solid state using KBr disc were performed in the range of 400–4000 cm<sup>-1</sup> with a Perkin-Elmer 1000 FTIR spectrometer. Elemental analyses (C,H and N) were performed using a Thermo FlashAE 1112 series analyzer. High-resolution electrospray ionization mass spectrometry (HR-ESI-TOF-MS) were recorded with a Bruker micrOTOF QII spectrometer equipped with an Apollo II ESI source. Ultraviolet-visible absorption spectra were recorded using a Spectronic GENESYS 6 UV-vis spectrophotometer (Thermo Electron Corporation) between 200–800 nm. Single crystal X-ray diffraction analyses were performed with an Oxford Gemini S diffractometer.

meso-5,10,15,20-Tetraphenylporphyrin (**H<sub>2</sub>TPP**),<sup>2</sup> copper(II)-5,10,15,20-tetraphenylporphyrin (**CuTPP**),<sup>3</sup> [ZnCl<sub>2</sub>·2thf],<sup>4</sup> [N(*n*Bu)<sub>4</sub>][B(C<sub>6</sub>F<sub>5</sub>)<sub>4</sub>],<sup>5</sup> and [P(*t*Bu)<sub>2</sub>C(CH<sub>3</sub>)<sub>2</sub>CH<sub>2</sub>Pd(μ-Cl)]<sub>2</sub><sup>6</sup> were prepared according to published procedures. Other chemicals were purchased from commercial suppliers and used without further purification. Aluminium oxide (Alumina: 90 neutral with activity grade of 1, particle size 50–200 μm and specific surface (BET) ≈ 130 m<sup>2</sup>/g) for column chromatography was purchased from MACHEREY-NAGEL GmbH & Co. KG; Germany. While preparative silica gel plates (silica gel G, 20 × 20 cm, 500 μm, Analtech uniplate) were bought from Sigma-Aldrich.

### 1.2 Synthesis and Analytical Data of H<sub>2</sub>TPP and CuTPP



Scheme S1. Synthesis of H<sub>2</sub>TPP and CuTPP.

## Synthesis of meso-5,10,15,20-tetraphenylporphyrin, **H<sub>2</sub>TPP**

According to reference (2), to a solution of benzaldehyde (6.641 g, 72 mmol) in propionic acid (300 mL), freshly distilled pyrrole (5.00 mL, 72 mmol) was added, and the reaction mixture was heated to reflux for 30 min. After cooling it to ambient temperature, the purple precipitate was filtered off and washed with hot distilled water (5 × 100 mL) followed by MeOH (3 × 30 mL). The product was then dried in an oven at 100 °C for 5 h and used without any further purification. Yield: 1.92 g (3.13 mmol, 20% based on benzaldehyde).

### Analytical Data of **H<sub>2</sub>TPP**

Elemental analysis (%) for C<sub>44</sub>H<sub>30</sub>N<sub>4</sub> (614.74 g/mol) calcd: C, 85.97; H, 4.92; N, 9.11; found: C, 85.63; H, 4.95; N, 9.05. <sup>1</sup>H NMR (CDCl<sub>3</sub>): δ ppm: -2.75 (s, 2H, N-H, H<sup>a,a'</sup>), 7.73–7.78 (m, 12H, *m*- and *p*-Ph-H, H<sup>1,2,2'</sup>), 8.21–8.23 (m, 8H, *o*-Ph-H, H<sup>3,3'</sup>), 8.85 (s, 8H, β-pyrrolic-H, H<sup>7,7'</sup>). <sup>13</sup>C NMR (CDCl<sub>3</sub>) δ ppm: 120.3 (C<sup>5</sup>), 126.8 (C<sup>2,2'</sup>), 127.9 (C<sup>1</sup>), 131.2 (br, C<sup>7,7'</sup>), 134.7 (C<sup>3,3'</sup>), 142.4 (C<sup>4</sup>).<sup>7</sup> IR (KBr, *v*, cm<sup>-1</sup>): 3317 (m, *v*<sub>N-H</sub>), 3054/3024 (m/m, *v*<sub>C-H</sub>),<sup>8</sup> 1596 (m), 1558 (w), 1491 (w), 1472 (m), 1441 (m), 1400 (w), 1350 (m), 1286 (w), 1251 (w), 1220 (m), 1176 (m), 1155 (w), 1071 (m), 1053 (w), 1031 (w), 1001 (m), 980 (m), 965 (s), 876 (w), 846 (w), 800 (s), 729 (s), 701 (s), 657 (m), 639 (w), 559 (w), 518 (w). HRMS (ESI-TOF): *m/z* calcd for: C<sub>44</sub>H<sub>31</sub>N<sub>4</sub>, 615.2543 [M+H]<sup>+</sup>; found: 615.2657. UV-vis (in CH<sub>2</sub>Cl<sub>2</sub>) λ<sub>abs</sub> [nm] (ε M<sup>-1</sup>cm<sup>-1</sup>) (at c = 2.1147·10<sup>-6</sup> M): 417 (≈ 426579), 514 (≈ 16218), 549 (≈ 6606), 589 (≈ 4466) and 645 (≈ 4073).<sup>9</sup> (See Figures S1, S2, S3 and S10 for <sup>1</sup>H, <sup>13</sup>C NMR, HR-ESI-TOF-MS, IR and UV-vis spectra of **H<sub>2</sub>TPP**, respectively).

## Synthesis of meso-5,10,15,20-tetraphenylporphyrinato-copper(II), **CuTPP**

To a solution of **H<sub>2</sub>TPP** (1.00 g, 1.6 mmol) in CHCl<sub>3</sub> (200 mL), a solution of Cu(OAc)<sub>2</sub>·H<sub>2</sub>O (1.62 g, 8.1 mmol) in MeOH (100 mL) was added in a single portion and the reaction mixture was heated to reflux for a 6 h. After cooling it to ambient temperature, the reaction mixture was transferred to a separatory funnel and washed thoroughly with a brine solution and distilled water to remove the excess of copper acetate. The organic phase was then dried over MgSO<sub>4</sub> and all the volatiles were removed with a rotary evaporator. The purple solid of **CuTPP** was dried in an oven at 100 °C for 5 h and used without further purification. Yield: 0.96 g (1.42 mmol, 87% based on **H<sub>2</sub>TPP**).

### Analytical Data of **CuTPP**

Elemental analysis (%) for C<sub>44</sub>H<sub>28</sub>CuN<sub>4</sub> (676.27 g/mol) calcd: C, 78.15; H, 4.17; N, 8.28; found: C, 78.36; H, 4.45; N, 8.34. IR (KBr, *v*, cm<sup>-1</sup>): 3054/3024 (m/w, *v*<sub>C-H</sub>), 1598 (m), 1576 (w), 1535 (w), 1516 (w), 1489 (m), 1441 (m), 1371 (w), 1345 (s), 1308 (w), 1206 (m), 1177 (m), 1157 (w), 1072 (m), 1005 (s), 835 (w), 795 (s), 743 (m), 699 (s), 661 (w), 523 (w). HRMS (ESI-TOF): *m/z* calcd for: C<sub>44</sub>H<sub>28</sub>CuN<sub>4</sub>/C<sub>44</sub>H<sub>29</sub>CuN<sub>4</sub>/C<sub>44</sub>H<sub>28</sub>CuKN<sub>4</sub>/C<sub>88</sub>H<sub>57</sub>Cu<sub>2</sub>N<sub>8</sub>/C<sub>88</sub>H<sub>56</sub>Cu<sub>2</sub>N<sub>8</sub>Na/C<sub>88</sub>H<sub>56</sub>CuKN<sub>8</sub>, 675.1604 [M]<sup>+</sup>/676.1683 [M+H]<sup>+</sup>/714.1242 [M+K]<sup>+</sup>/1351.3273 [2M+H]<sup>+</sup>/1373.3152 [2M+Na]<sup>+</sup>/1389.2951 [2M+K]<sup>+</sup>, found: 675.1600 / 676.1669 / 714.1248 / 1351.3204 / 1373.3122 / 1389.2953. UV-vis (in CH<sub>2</sub>Cl<sub>2</sub>) λ<sub>abs</sub> [nm] (ε M<sup>-1</sup>cm<sup>-1</sup>) (at c = 3.1053·10<sup>-6</sup> M): 415 (≈ 331131), 539 (≈ 13183) and 617 (≈ 1000).<sup>10</sup> (See Figures S4, S5 and S11 for HR-ESI-TOF-MS, IR and UV-vis spectra of **CuTPP**, respectively).

### 1.3 Synthesis and Analytical Data of $\text{CuTPPBr}_8 \cdot \text{CHCl}_3$ and $\{\text{TPPFc}_8(\text{H}_2\text{O})_2\}$

Synthesis of  $\beta$ -2,3,7,8,12,13,17,18-octabromo-meso-5,10,15,20-tetraphenylporphyrinato-copper(II), **CuTPPBr<sub>8</sub>·CHCl<sub>3</sub>**

To a solution of **CuTPP** (0.80 g, 1.18 mmol) in  $\text{CHCl}_3$  (100 mL), N-bromosuccinamide (10.00 g, 56.19 mmol) was added in a single portion and the reaction mixture was heated at reflux for 16 h. Afterward, a further amount of N-bromosuccinamide (3.00 g, 16.86 mmol) was added and the reaction mixture was heated at reflux for 24 h. After that, alumina ( $\approx 4$  g) was added and all volatiles were removed under reduced pressure (**Crude-1**). The obtained residue was loaded on an alumina column ( $3 \times 25$  cm) for purification (see Scheme S2). Pure **CuTPPBr<sub>8</sub>** in form of the adduct **CuTPPBr<sub>8</sub>·CHCl<sub>3</sub>** was obtained as a deep-green solid in a yield of 1.1-1.3 g (0.77–0.91 mmol, 65–77%, based on **CuTPP**).

Analytical Data of **CuTPPBr<sub>8</sub>·CHCl<sub>3</sub>**

Elemental analysis (%) for  $\text{C}_{44}\text{H}_{20}\text{Br}_8\text{CuN}_4 \cdot \text{CHCl}_3$  (1426.81 g/mol) calcd: C 37.88, H 1.48, N 3.93; found: C 37.97, H 1.45, N 3.96. IR (KBr,  $\nu$ ,  $\text{cm}^{-1}$ ): 3054/3021 (w/w,  $\nu_{\text{C-H}}$ ), 1442 (w), 1408 (w), 1319 (m), 1244 (w), 1178 (w), 1156 (w), 1065 (w), 1039 (m), 1023 (s), 923 (m), 838 (w), 752 (m), 734 (m), 695 (m), 656 (w). HRMS (ESI-TOF):  $m/z$  calcd for:  $\text{C}_{44}\text{H}_{21}\text{Br}_8\text{CuN}_4/\text{C}_{88}\text{H}_{41}\text{Br}_{16}\text{Cu}_2\text{N}_8/\text{C}_{88}\text{H}_{40}\text{Br}_{16}\text{Cu}_2\text{KN}_8$ , 1307.4438  $[\text{M}+\text{H}]^+$  /2615.8822  $[\text{2M}+\text{H}]^+/\text{2653.8381}$   $[\text{2M}+\text{K}]^+$ , found: 1307.4449/2615.8720/2653.8469. UV-vis (in  $\text{CH}_2\text{Cl}_2$ )  $\lambda_{\text{abs}}$  [nm] ( $\epsilon$   $\text{M}^{-1}\text{cm}^{-1}$ ) (at  $c = 8.7959 \cdot 10^{-6}$  M): 446 (sh) ( $\approx 128825$ ), 465 ( $\approx 144544$ ), 581 ( $\approx 17783$ ) and 624 ( $\approx 6607$ ).<sup>11</sup> (See Figures S6, S7 and S12 for HR-ESI-TOF-MS, IR and UV-vis spectra of **CuTPPBr<sub>8</sub>·CHCl<sub>3</sub>**, respectively).

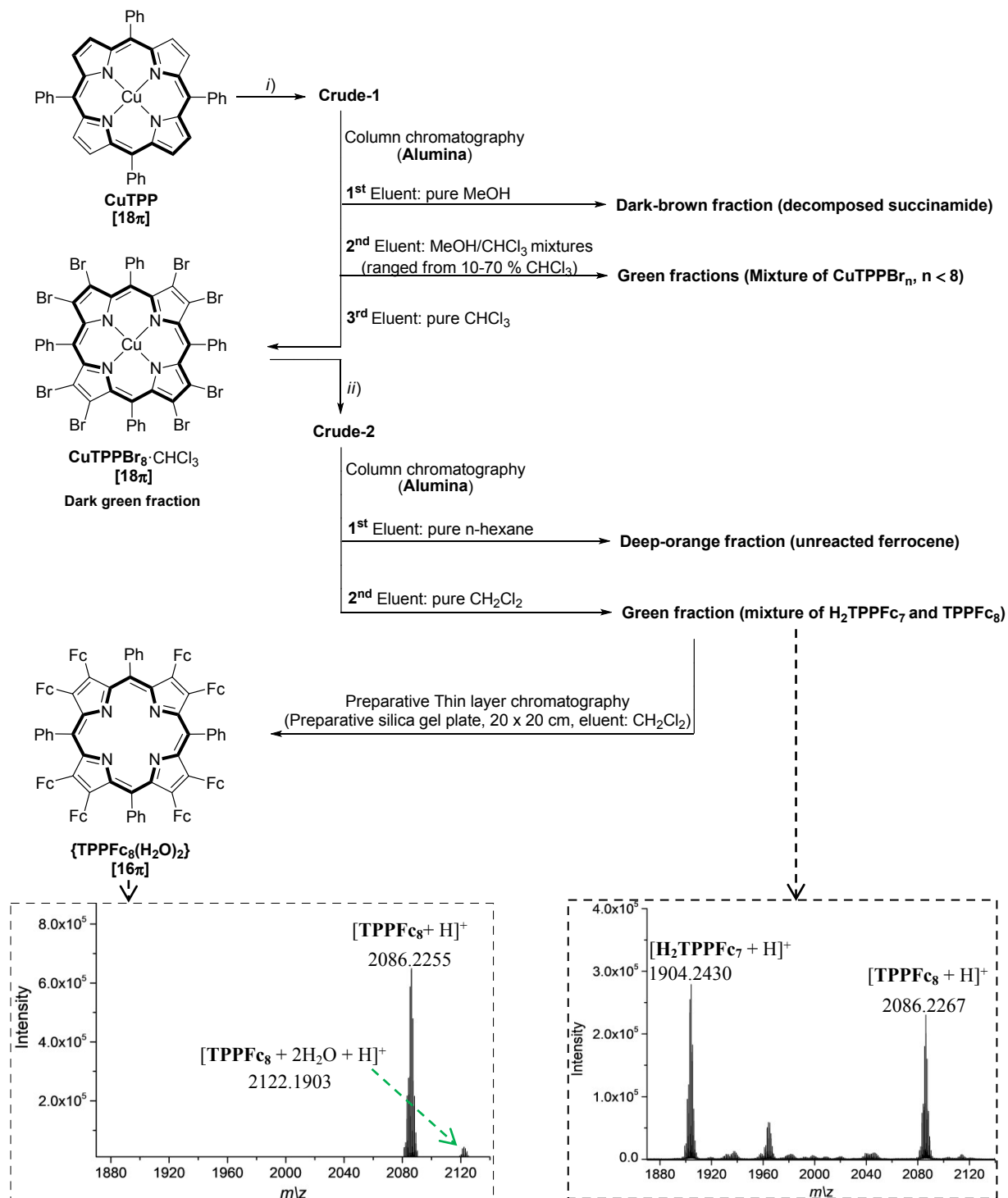
Synthesis of diaquo- $\beta$ -2,3,7,8,12,13,17,18-octaferrocenyl-meso-5,10,15,20-tetraphenylporphyrin,  $\{\text{TPPFc}_8(\text{H}_2\text{O})_2\}$

To a solution of ferrocene (0.9107 g, 4.89 mmol) and  $\text{KO}t\text{Bu}$  (0.0547 g, 0.49 mmol) in anhydrous THF (100 mL) at  $-78$  °C,  $t\text{BuLi}$  (3.90 mL, 1.9 M in n-pentane) was added dropwise *via* a syringe within 5 min. The reaction mixture was stirred for 1 h at  $-78$  °C. After that, the reaction mixture was warmed to  $-50$  °C and  $[\text{ZnCl}_2 \cdot 2\text{thf}]$  (2.20 g, 7.83 mmol) was added in a single portion and the reaction mixture was stirred at  $-50$  °C for 1 h. Then it was allowed to warm to ambient temperature and stirring was continued for 1 h. Afterward, **CuTPPBr<sub>8</sub>·CHCl<sub>3</sub>** (0.200 g, 0.140 mmol) and  $[\text{P}(t\text{Bu})_2\text{C}(\text{CH}_3)_2\text{CH}_2\text{Pd}(\mu\text{-Cl})_2]$  (0.0423 g, 0.0616 mmol) were added in single portions. The flask was closed and under solvothermal reaction conditions it was heated to 95 °C for 24 h. A second portion of  $[\text{P}(t\text{Bu})_2\text{C}(\text{CH}_3)_2\text{CH}_2\text{Pd}(\mu\text{-Cl})_2]$  (0.0347 g, 0.0505 mmol) was added after cooling down to ambient temperature and the solvothermal heating was repeated as above. After cooling down to ambient temperature all volatiles were removed under reduced pressure, and the crude product (**Crude-2**) was worked up by column chromatography (column-size:  $3 \times 10$  cm, alumina). The 1<sup>st</sup> fraction contained unreacted ferrocene which was isolated using n-hexane as eluent, while the 2<sup>nd</sup> fraction using  $\text{CH}_2\text{Cl}_2$  as eluent, contained the title compound **TPPFc<sub>8</sub>** contaminated with *hepta*-ferrocenylated **H<sub>2</sub>TPPFc<sub>7</sub>**. After performing a thin layer chromatography (preparative silica gel layer,  $20 \times 20$  cm, 500 microns) using  $\text{CH}_2\text{Cl}_2$  as eluent, **TPPFc<sub>8</sub>** could be isolated after evaporation of the solvent in form of  $\{\text{TPPFc}_8(\text{H}_2\text{O})_2\}$  as a green solid in yields between 26 to 32 mg (9–11%, based on **CuTPPBr<sub>8</sub>·CHCl<sub>3</sub>**). The synthesis and purification procedure to obtain **CuTPPBr<sub>8</sub>·CHCl<sub>3</sub>** and  $\{\text{TPPFc}_8(\text{H}_2\text{O})_2\}$  in a pure state is summarized in Scheme S2.

### Analytical Data of {TPPFc<sub>8</sub>(H<sub>2</sub>O)<sub>2</sub>}

IR (KBr,  $\nu$ , cm<sup>-1</sup>): 3090 (w,  $\nu_{C-H}$ ), 2957 (w), 2923 (m), 2852 (w), 1661 (w), 1640 (w), 1469 (w), 1444 (w), 1412 (w), 1386 (w), 1333 (w), 1307 (w), 1260 (m), 1237 (w), 1197 (w), 1105/1003 (m/m),<sup>12</sup> 938 (m), 857 (w), 814 (s,  $\gamma_{Fe-H}$ , out of plane bending vibration), 738 (m), 693 (m), 596 (w). HRMS (ESI-TOF):  $m/z$  calcd for: C<sub>124</sub>H<sub>93</sub>Fe<sub>8</sub>N<sub>4</sub>/C<sub>124</sub>H<sub>97</sub>Fe<sub>8</sub>N<sub>4</sub>O<sub>2</sub>/C<sub>125</sub>H<sub>95</sub>Cl<sub>2</sub>Fe<sub>8</sub>N<sub>4</sub>Na, 2086.2238 [M+H]<sup>+</sup>/ 2122.2449 [M+2H<sub>2</sub>O+H]<sup>+</sup>/2193.1571 [M+CH<sub>2</sub>Cl<sub>2</sub>+Na+H]<sup>+</sup>; found: 2086.2255/2122.1903/2193.1147. UV-vis (in CH<sub>2</sub>Cl<sub>2</sub>)  $\lambda_{abs}$  [nm] ( $\epsilon$  M<sup>-1</sup>cm<sup>-1</sup>) ( at c = 4.9644.10<sup>-6</sup> M): 230 ( $\approx$  263027), 362 ( $\approx$  117489) (See Figures S8, S9 and S13 for HR-ESI-TOF-MS, IR and UV-vis spectra of {TPPFc<sub>8</sub>(H<sub>2</sub>O)<sub>2</sub>} , respectively).

## 1.4 Purification of $\text{CuTPPBr}_8 \cdot \text{CHCl}_3$ and $\{\text{TPPFc}_8(\text{H}_2\text{O})_2\}$



**Scheme S2.** Synthesis and purification of  $\text{CuTPPBr}_8 \cdot \text{CHCl}_3$  and  $\{\text{TPPFc}_8(\text{H}_2\text{O})_2\}$ : *i*) N-bromosuccinamide,  $\text{CHCl}_3$ , reflux 40 h, *ii*) 1<sup>st</sup>: Ferrocene,  $\text{KO}t\text{Bu}$ , THF,  $t\text{BuLi}$ ,  $-78^\circ\text{C}$ , 1 h; 2<sup>nd</sup>:  $[\text{ZnCl}_2 \cdot 2\text{thf}]$ ,  $-50^\circ\text{C}$ , 1 h,  $25^\circ\text{C}$ , 1 h; 3<sup>rd</sup>:  $[\text{P}(t\text{Bu})_2\text{C}(\text{CH}_3)_2\text{CH}_2\text{Pd}(\mu\text{-Cl})_2]$ ,  $95^\circ\text{C}$ , 48 h. The HR-ESI-TOF-MS spectra refer to the obtained mixture of  $\text{H}_2\text{TPPFc}_7$  and  $\text{TPPFc}_8$  (right), and pure  $\{\text{TPPFc}_8(\text{H}_2\text{O})_2\}$  after additional purification (left).

### 1.4.1 Comments to the synthesis and isolation of $\{\text{TPPFc}_8(\text{H}_2\text{O})_2\}$

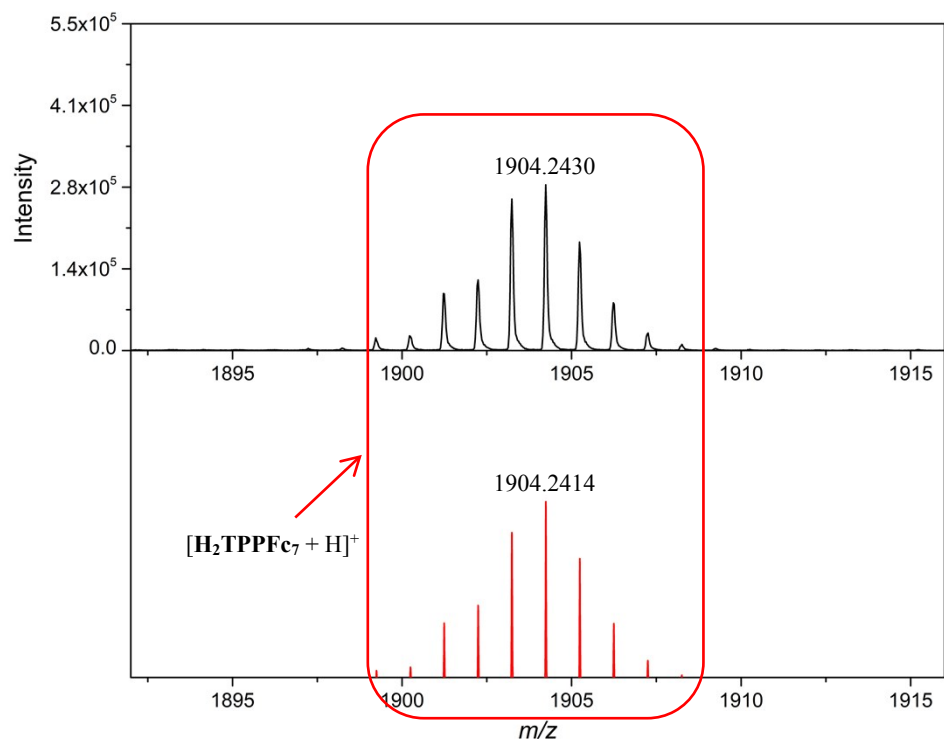
After column chromatography of **Crude-2** with  $\text{CH}_2\text{Cl}_2$ , green fractions were obtained of which ESI-TOF-MS measurements revealed the formation/presence of both  $\text{H}_2\text{TPPFc}_7$  and  $\text{TPPFc}_8$  (Scheme 2). According to the ESI-TOF-MS spectra displayed in Scheme 2 and below in Scheme S2a we attribute  $\text{H}_2\text{TPPFc}_7$  to a  $18\pi$  porphyrin, although we could not isolate sufficient material for further analysis. At that stage  $\text{TPPFc}_8$  is obviously free of water, as the before-mentioned ESI-TOF-MS measurements did never reveal the presence of water. However, after the preparative thin layer chromatography and all required manipulations performed under aerobic working conditions the ESI-TOF-MS measurements reveal the presence of two water molecules. The presence and the nature of interaction of these two water molecules was (further) confirmed by a single crystal X-ray crystallographic study. Due to this we assigned the title compound as  $\{\text{TPPFc}_8(\text{H}_2\text{O})_2\}$ . For all analytical measurements crystals of  $\{\text{TPPFc}_8(\text{H}_2\text{O})_2\}$  were used.

The conversion of  $\text{CuTPPBr}_8$  to  $\{\text{TPPFc}_8(\text{H}_2\text{O})_2\}$  was performed under anaerobic working conditions. The intense dark-green colour of the reaction solution observed after the addition of  $\text{CuTPPBr}_8$  modified by time to green only. After the end of the reaction and evaporation of all volatiles a green solid was obtained. All subsequent operations were performed under air and/or in  $\text{CH}_2\text{Cl}_2$  solutions, whereby no further colour changes could be noticed. Furthermore,  $\{\text{TPPFc}_8(\text{H}_2\text{O})_2\}$  was crystallized out of  $\text{CH}_2\text{Cl}_2$ :DMF (v:v = 40:1) solutions against n-hexane in a closed system but under aerobic conditions. By time  $\text{CH}_2\text{Cl}_2$  did slowly evaporate and due to the complete crystallization of  $\{\text{TPPFc}_8(\text{H}_2\text{O})_2\}$  the  $\text{CH}_2\text{Cl}_2$  became colourless. Under the microscope we exclusively observed the formation of purple plates. These observations and the in Chapter 2.4 (see below) reported UV-vis measurements of  $\{\text{TPPFc}_8(\text{H}_2\text{O})_2\}$  demonstrate that this compound is not air and/or moisture sensitive, as reported for  $16\pi$  OiPTPP.<sup>20</sup> In addition, these observations tells that the low yield of  $\{\text{TPPFc}_8(\text{H}_2\text{O})_2\}$  is not due to a (partial) decomposition during the aerobic work-up.

The question arises why the  $16\pi$   $\text{TPPFc}_8$  was formed out of  $\text{CuTPPBr}_8$  during a Negishi *C,C* cross coupling. So far,  $16\pi$  porphyrins were synthesized by the addition of  $\text{SbCl}_5$  as oxidizing agent to  $\text{CH}_2\text{Cl}_2$  solutions of  $18\pi$  porphyrins.<sup>20</sup> and references therein The question is thus, which chemical species acted as an oxidizing agent in the here reported case. The situation is further complicated as in due course of our reaction –Br substituents were replaced by Ferrocenyl groups. In order to oxidize first and to substitute –Br vs –Fc second, we tried to oxidize  $\text{CuTPPBr}_8$  with  $\text{SbCl}_5$  in  $\text{CH}_2\text{Cl}_2$  solutions, according to reference.<sup>20</sup> In such cases we observed the precipitation of insoluble and black-coloured material only. It remains speculative whether  $[\text{P}(t\text{Bu})_2\text{C}(\text{CH}_3)_2\text{CH}_2\text{Pd}(\mu\text{-Cl})_2]$  might be responsible for both the –Br vs –Fc substitution and the oxidation. With the catalyst itself we have good experiences and could describe several times its applicability for Negishi *C,C* cross couplings.<sup>13-15</sup> By reducing the amount of the catalyst to the half and less in the here reported case we did observe the formation of  $16\pi$   $\text{TPPFc}_8$ , while doubling its amount did not give rise to higher yields of  $16\pi$   $\text{TPPFc}_8$ .

We can thus not answer this final question but aim to indicate that we investigating the reaction of other  $18\pi$  and octabromo-porphyrins with different catalysts for *C,C* cross coupling reactions.





**Scheme S2a.** HR-ESI-TOF-MS spectrum of  $\text{H}_2\text{TPPFc}_7$  (Black: measured in  $\text{CH}_2\text{Cl}_2$  as part of the green fraction reported in Scheme 2, red: calculated).

## 1.5 $^1\text{H}$ and $^{13}\text{C}$ NMR spectra of $\text{H}_2\text{TPP}$

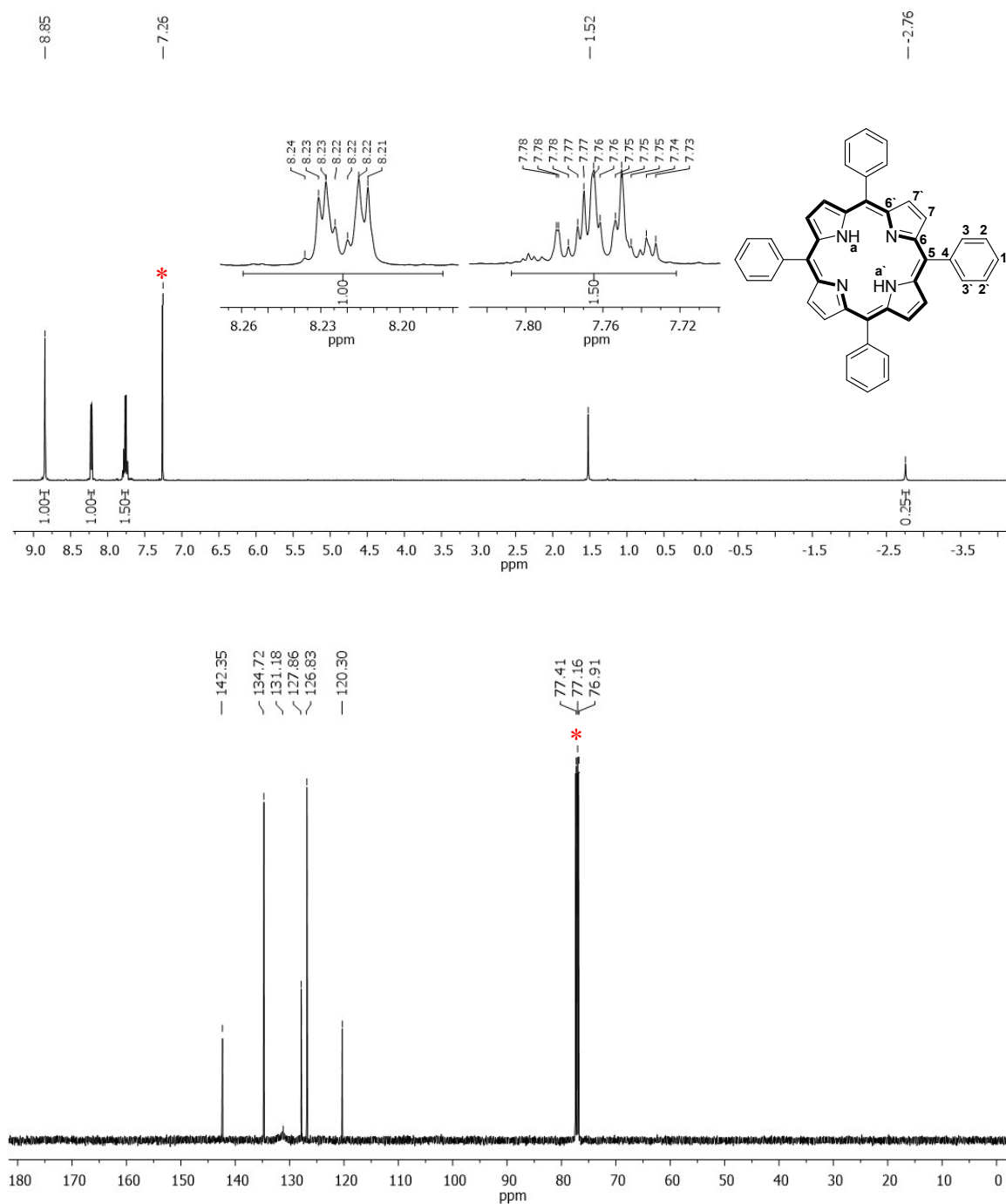


**Figure S1.**  $^1\text{H}$  (above) and  $^{13}\text{C}$  NMR spectra (below) of  $\text{H}_2\text{TPP}$  in  $\text{CDCl}_3$

1) According to Manke et al.<sup>16</sup> the  $^{13}\text{C}$  NMR resonances of pyrrole carbon atoms are not observable.

## 1.6 HR-ESI-TOF-MS and IR spectra of H<sub>2</sub>TPP

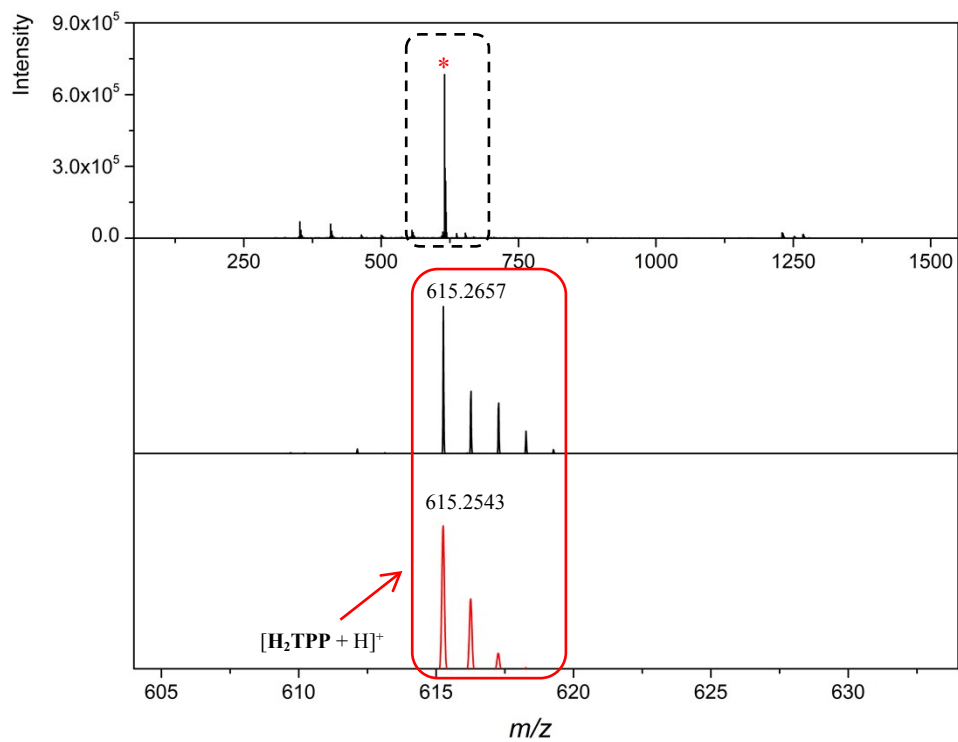


**Figure S2.** HR-ESI-TOF-MS spectrum of H<sub>2</sub>TPP (black: measured in (CH<sub>2</sub>Cl<sub>2</sub>/CH<sub>3</sub>CN), red: calculated).

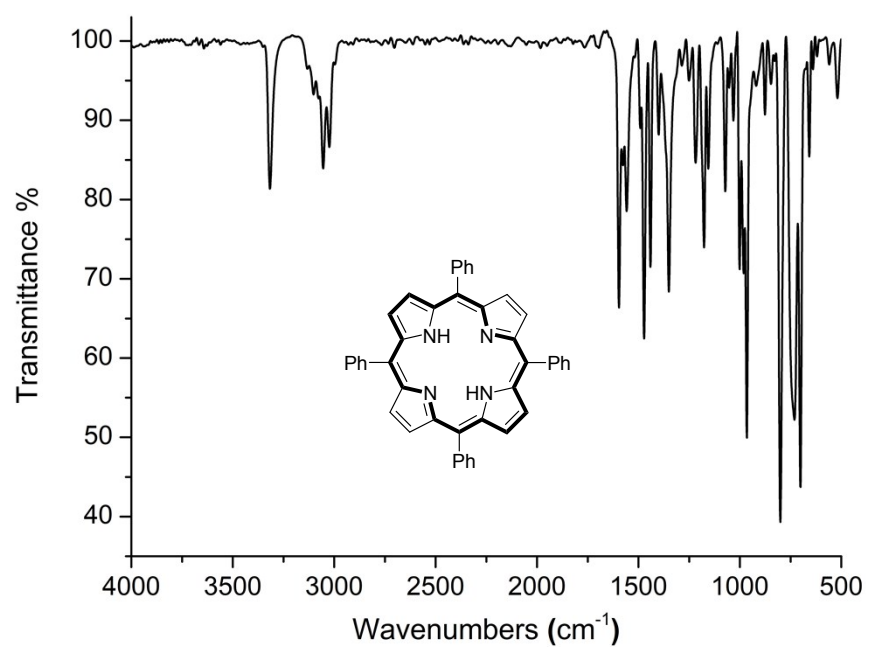


**Figure S3.** IR spectrum (KBr) of H<sub>2</sub>TPP.

## 1.7 HR-ESI-TOF-MS and IR spectra of CuTPP

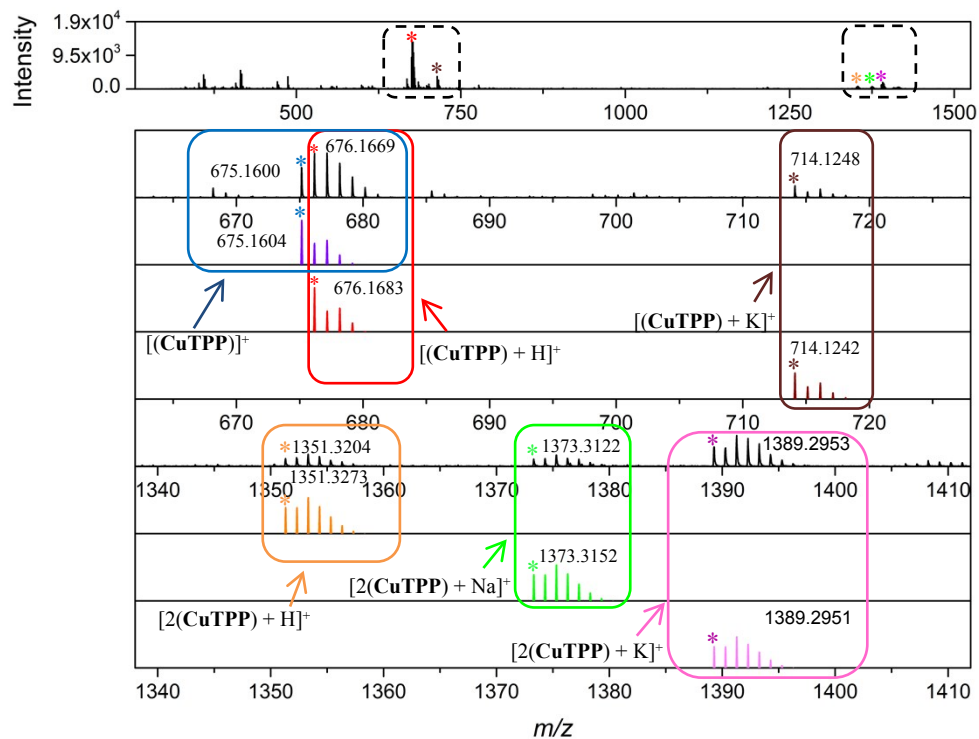


**Figure S4.** HR-ESI-TOF-MS spectrum of CuTPP (black: measured in (CH<sub>2</sub>Cl<sub>2</sub>/CH<sub>3</sub>CN), red: calculated).

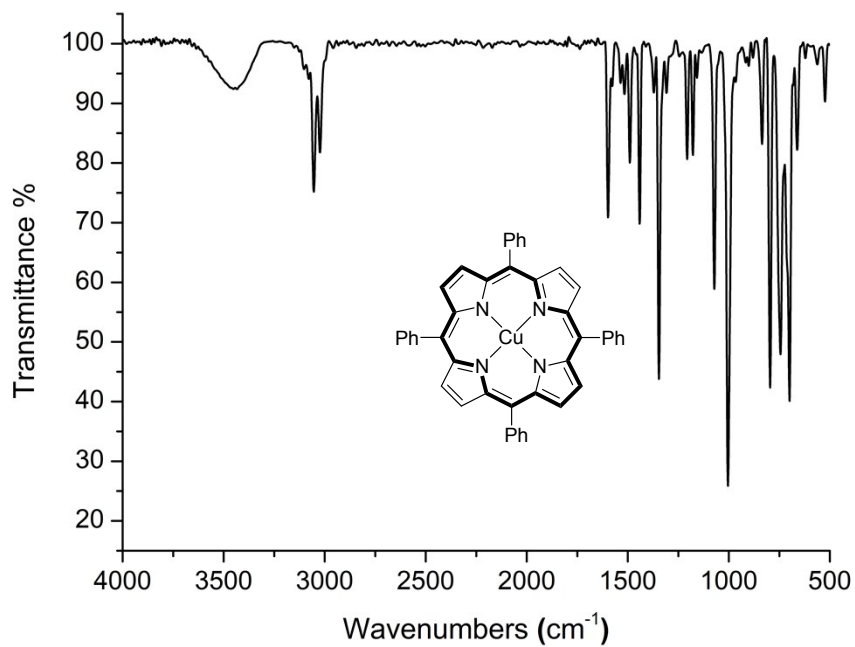


**Figure S5.** IR spectrum (KBr) of CuTPP.

## 1.8 HR-ESI-TOF-MS and IR spectra of $\text{CuTPPBr}_8 \cdot \text{CHCl}_3$

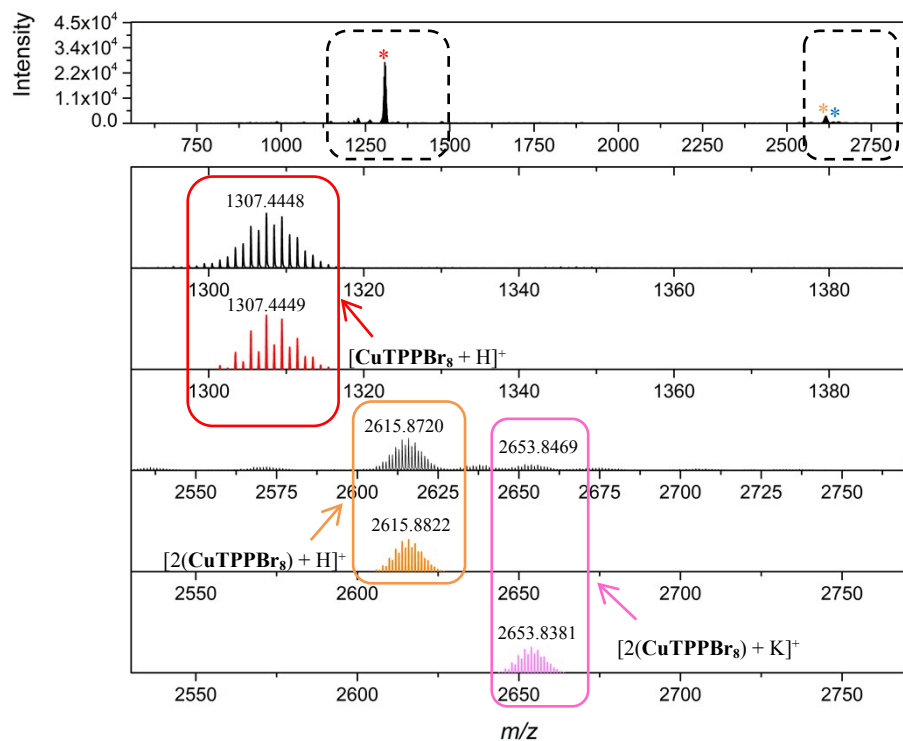


**Figure S6.** HR-ESI-TOF-MS spectrum of  $\text{CuTPPBr}_8 \cdot \text{CHCl}_3$  (black: measured in  $(\text{CH}_2\text{Cl}_2/\text{CH}_3\text{CN})$ , red, orange and purple: calculated).

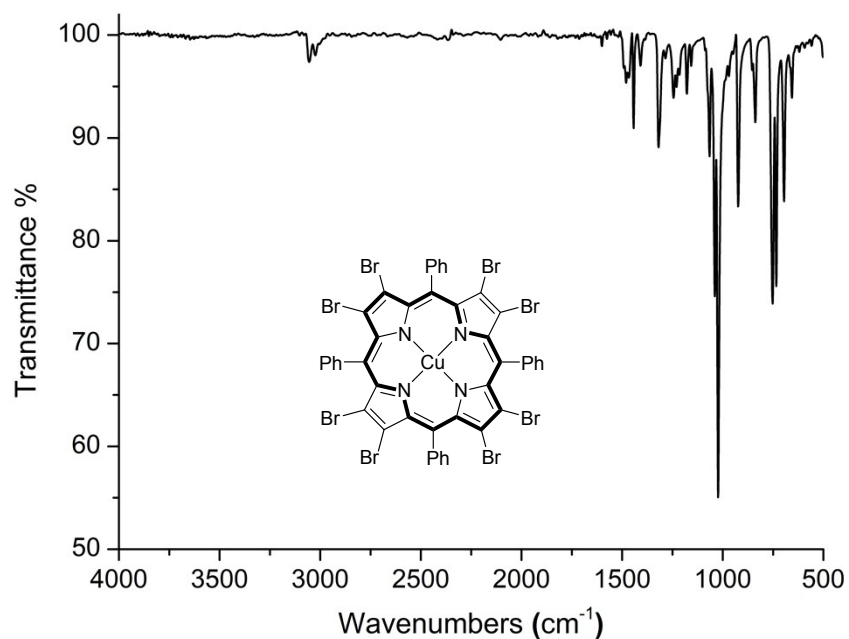


**Figure S7.** IR spectrum (KBr) of  $\text{CuTPPBr}_8 \cdot \text{CHCl}_3$ .

## 1.9 HR-ESI-TOF-MS and IR spectra of $\{\text{TPPFc}_8(\text{H}_2\text{O})_2\}$

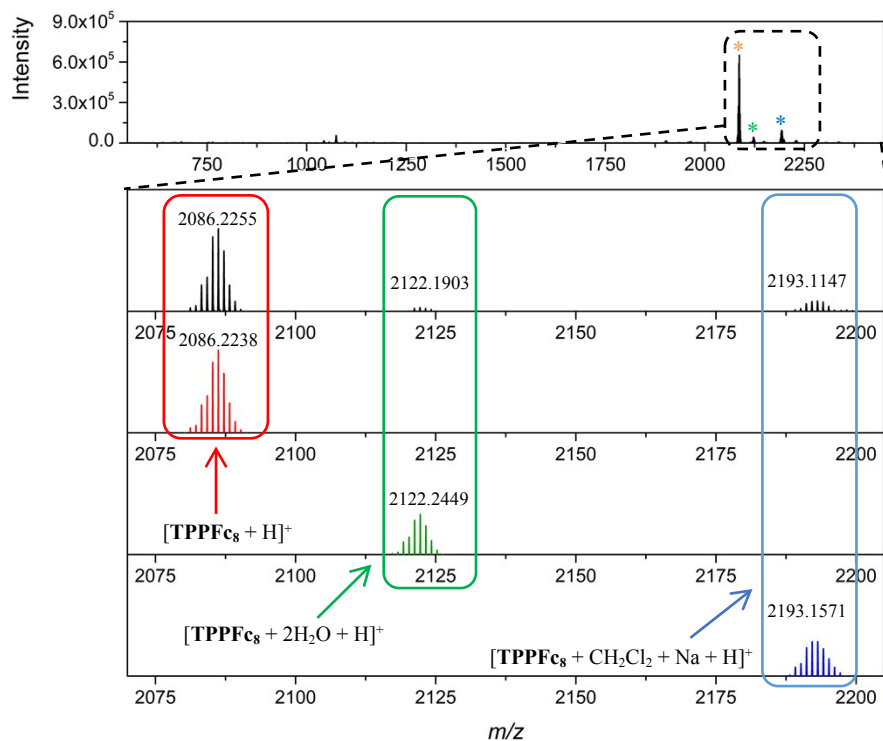


**Figure S8.** HR-ESI-TOF-MS spectrum of  $\{\text{TPPFc}_8(\text{H}_2\text{O})_2\}$  (black: measured in  $(\text{CH}_2\text{Cl}_2/\text{CH}_3\text{CN})$ , red, green and blue: calculated).

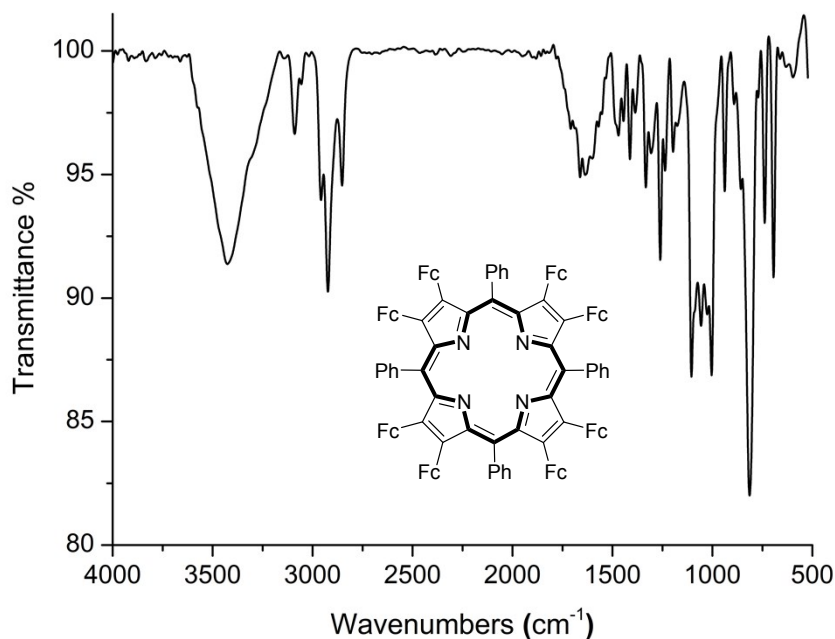


**Figure S9.** IR spectrum (KBr) of  $\{\text{TPPFc}_8(\text{H}_2\text{O})_2\}$ . According to the 1100 and 1000  $\text{cm}^{-1}$  rule of Rosenblum,<sup>12</sup> both bands are observed in the IR spectra of ferrocene derivatives when one of the Cp ( $\eta^5\text{-C}_5\text{H}_5$ ) rings is unsubstituted. This IR spectrum was measured out of isolated single crystals obtained by the diffusion controlled crystallization of  $\text{CH}_2\text{Cl}_2/\text{DMF}$  (v:v = 40:1) solution against n-hexane. Crystals were isolated by filtration and washed with n-hexane ( $2 \times 3$  mL) and dried in vacuo. Despite this, the IR spectrum display remaining amounts of  $\text{CH}_2\text{Cl}_2$  as packing solvent and DMF adsorbed at the crystals surface.

## 2. UV-vis absorption spectra

### 2.1 Concentration dependent UV-vis spectra of H<sub>2</sub>TPP

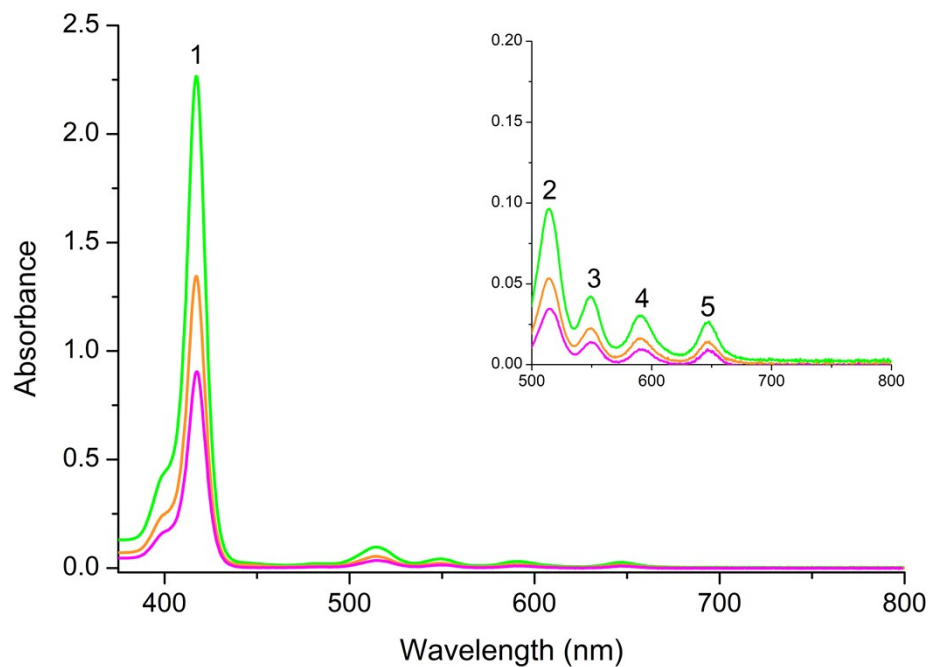


**Figure S10.** UV-vis spectrum of H<sub>2</sub>TPP in CH<sub>2</sub>Cl<sub>2</sub> (inserts is corresponding to the enlarged spectral range of 500–800 nm).

**Table S1.** UV-vis data for H<sub>2</sub>TPP in CH<sub>2</sub>Cl<sub>2</sub>

	Absorption $\lambda_{\max}$ [nm] log ( $\epsilon$ [ M <sup>-1</sup> cm <sup>-1</sup> ])				
	Soret (B) Band		Q Bands		
	1	2	3	4	5
<b>C1</b> = 5.2868.10 <sup>-6</sup>	417 (5.63)	514 (4.26)	549 (3.90)	589 (3.75)	645 (3.68)
<b>C2</b> = 3.1721.10 <sup>-6</sup>	417 (5.63)	514 (4.23)	549 (3.85)	589 (3.70)	645 (3.64)
<b>C3</b> = 2.1147.10 <sup>-6</sup>	417 (5.63)	514 (4.21)	549 (3.82)	589 (3.65)	646 (3.61)

## 2.2 Concentration-dependent UV-vis spectra of CuTPP

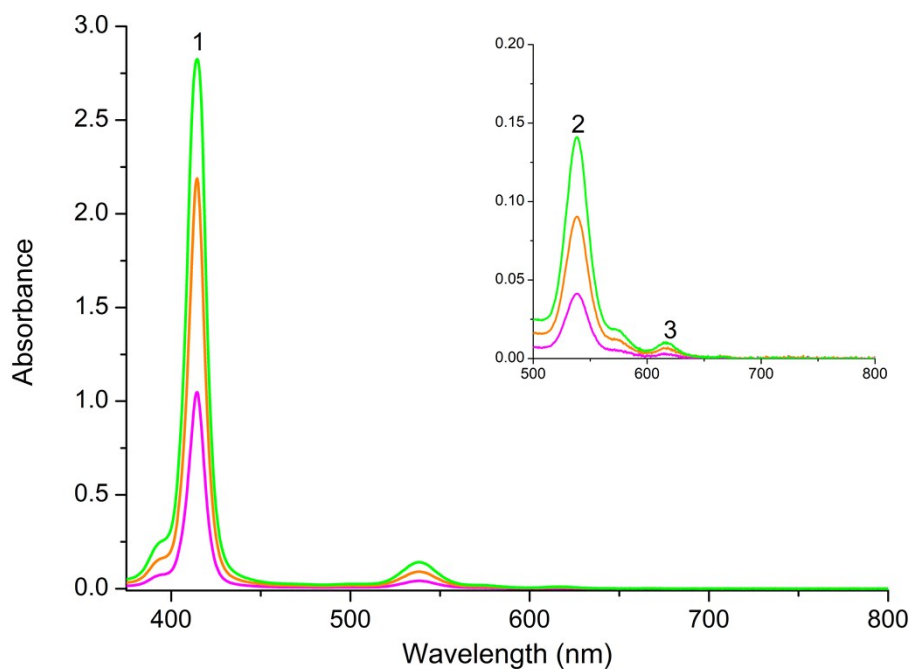


**Figure S11.** UV-vis spectrum of **CuTPP** in  $\text{CH}_2\text{Cl}_2$  (inserts is corresponding to the enlarged spectral range of 500–800 nm).

**Table S2.** UV-vis data for **CuTPP** in  $\text{CH}_2\text{Cl}_2$

	Absorption $\lambda_{\text{max}}$ [nm] $\log(\epsilon [\text{M}^{-1}\text{cm}^{-1}])$		
	Soret (B) Band		Q Bands
	1	2	3
<b>C1</b> = $7.7632 \cdot 10^{-6}$	415 (5.56)	539 (4.26)	617 (3.13)
<b>C2</b> = $6.2106 \cdot 10^{-6}$	415 (5.54)	539 (4.16)	617 (3.01)
<b>C3</b> = $3.1053 \cdot 10^{-6}$	415 (5.52)	539 (4.12)	617 (3.00)



### 2.3 Concentration dependent UV-vis spectra of $\text{CuTPPBr}_8 \cdot \text{CHCl}_3$

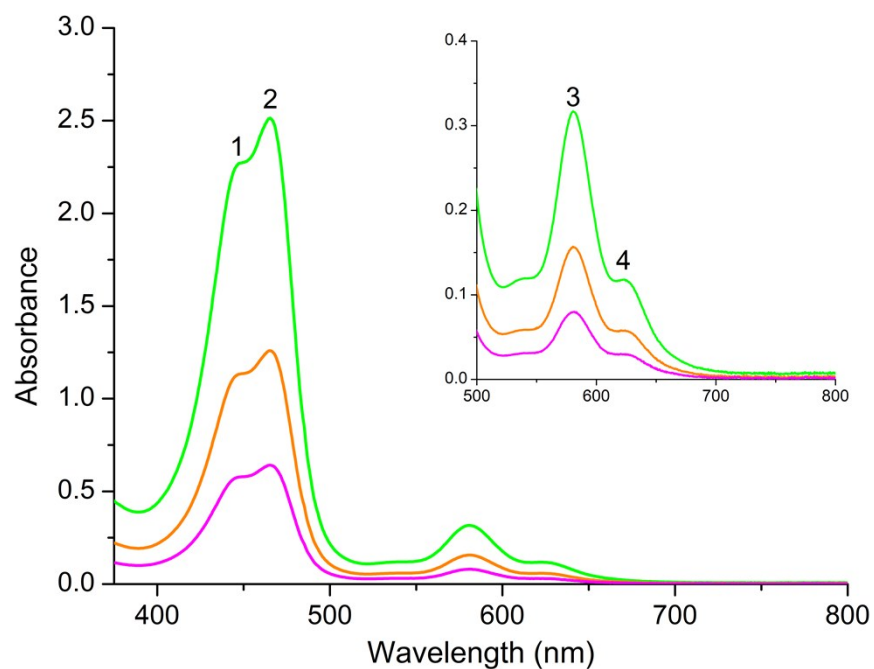


**Figure S12.** UV-vis spectrum of  $\text{CuTPPBr}_8 \cdot \text{CHCl}_3$  in  $\text{CH}_2\text{Cl}_2$  (inserts is corresponding to the enlarged spectral range of 500–800 nm).

**Table S3.** UV-vis data for  $\text{CuTPPBr}_8 \cdot \text{CHCl}_3$  in  $\text{CH}_2\text{Cl}_2$

	Absorption $\lambda_{\text{max}}$ [nm] log ( $\epsilon$ [ $\text{M}^{-1}\text{cm}^{-1}$ ])			
	Soret (B) Band		Q Bands	
	1	2	3	4
<b>C1</b> = $1.7592 \cdot 10^{-5}$	446(sh) (5.11)	465 (5.16)	581 (4.26)	624 (3.83)
<b>C2</b> = $8.7959 \cdot 10^{-6}$	446(sh) (5.11)	465 (5.16)	581 (4.25)	624 (3.82)
<b>C3</b> = $4.3979 \cdot 10^{-6}$	446(sh) (5.12)	465 (5.16)	581 (4.26)	624 (3.83)

## 2.4 Concentration-dependent UV-vis spectra of {TPPFc<sub>8</sub>(H<sub>2</sub>O)<sub>2</sub>}

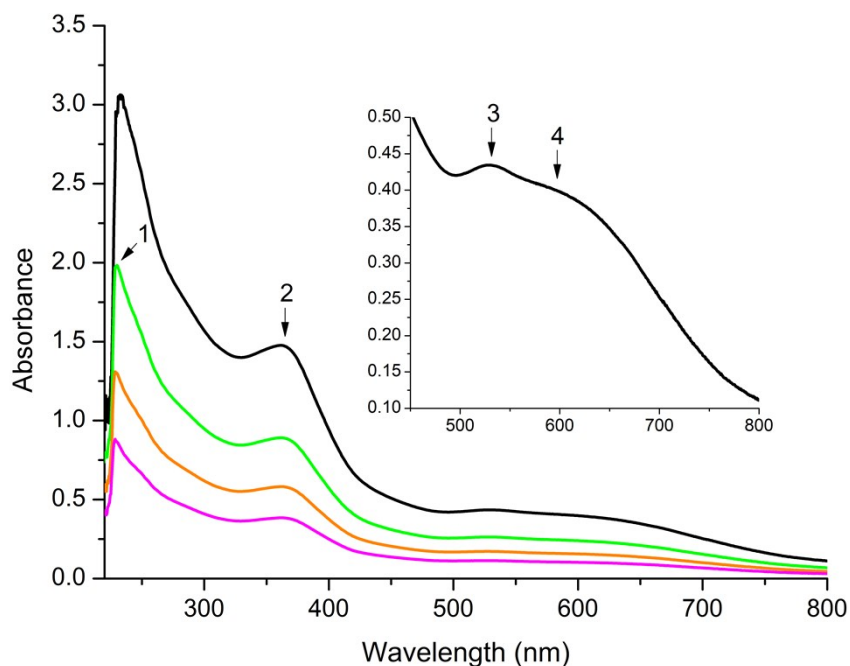


**Figure S13.** UV-vis spectrum of {TPPFc<sub>8</sub>(H<sub>2</sub>O)<sub>2</sub>} in CH<sub>2</sub>Cl<sub>2</sub> (insert is corresponding to the enlarged spectral range of 490–800 nm).

Comment: In order to analyze the absorptions No. 3 and 4 reliable, the UV-vis measurements were started with a comparatively high concentration. For this initial concentration we do not give  $\lambda$  and  $\epsilon$  values for the absorption No. 1 as the absorbance exceeds 3.0. All operations were performed under aerobic conditions, incl. the dilution of the original higher concentrated solution. These measurements took about 3 h. As the features of the UV-vis spectra did not change within this time-window we can rule out that this compound is not air and/or moisture sensitive.

**Table S4.** UV-vis data for {TPPFc<sub>8</sub>(H<sub>2</sub>O)<sub>2</sub>} in CH<sub>2</sub>Cl<sub>2</sub>

	Absorption $\lambda_{\max}$ [nm] log ( $\epsilon$ [ M <sup>-1</sup> cm <sup>-1</sup> ])			
	1	2	3	4
<b>C1</b> = 1.1032.10 <sup>-5</sup>	-	362 (5.13)	529 (4.60)	597 (3.62)
<b>C2</b> = 7.1708.10 <sup>-6</sup>	230 (5.44)	362 (5.06)	-	-
<b>C3</b> = 4.9644.10 <sup>-6</sup>	230 (5.42)	362 (5.07)	-	-
<b>C4</b> = 3.3096.10 <sup>-6</sup>	230 (5.41)	362 (5.06)	-	-

### 3. Electrochemical Measurements

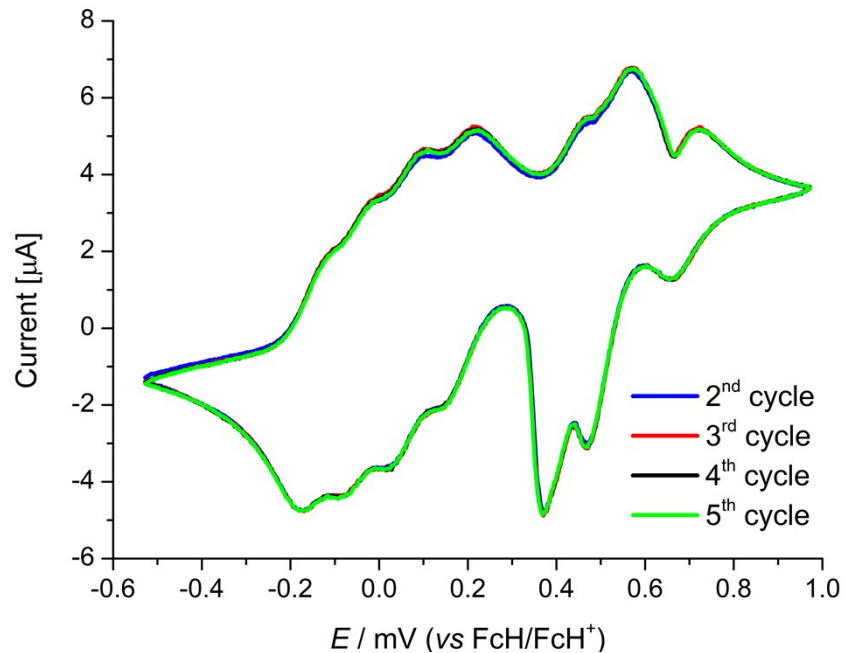


**Figure S14.** Set of cyclic voltammograms of  $\{\text{TPPFc}_8(\text{H}_2\text{O})_2\}$  in  $\text{CH}_2\text{Cl}_2$  ( $0.5 \text{ mmol}\cdot\text{L}^{-1}$ ) at rising potential to +1000 mV (vs. FcH/FcH<sup>+</sup>) at 25 °C, supporting electrolyte  $0.1 \text{ mol}\cdot\text{L}^{-1}$   $[\text{N}(\textit{n}\text{Bu})_4][\text{B}(\text{C}_6\text{F}_5)_4]$ , platinum working electrode. Decamethyl ferrocene was used as an internal reference.

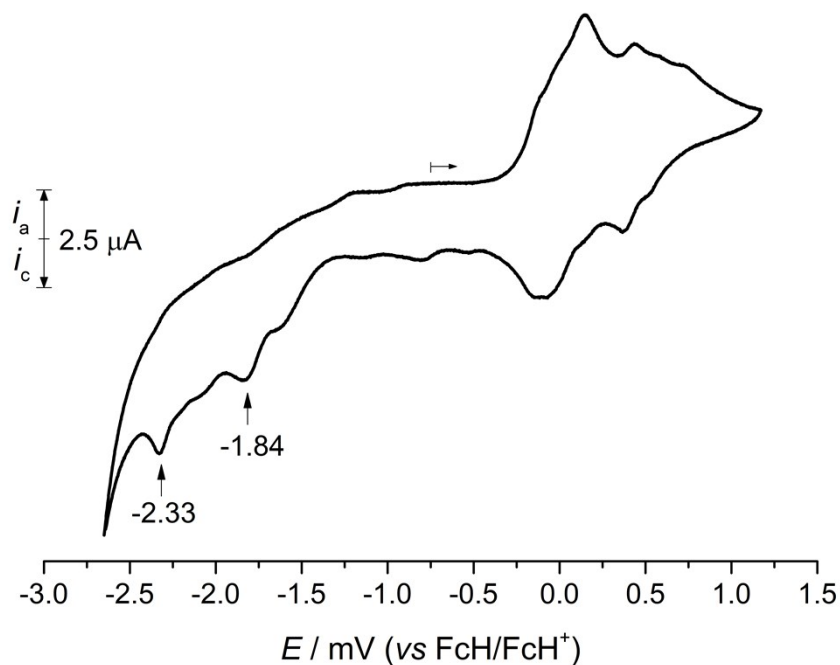


**Figure S15.** Cyclic voltammogram of  $\{\text{TPPFc}_8(\text{H}_2\text{O})_2\}$  in  $\text{CH}_2\text{Cl}_2$  ( $0.5 \text{ mmol}\cdot\text{L}^{-1}$ ) at rising potential from -2500 mV to +1400 mV (vs. FcH/FcH<sup>+</sup>) at 25 °C, supporting electrolyte  $0.1 \text{ mol}\cdot\text{L}^{-1}$   $[\text{N}(\textit{n}\text{Bu})_4][\text{B}(\text{C}_6\text{F}_5)_4]$ , platinum working electrode. Decamethyl ferrocene was used as an internal reference.

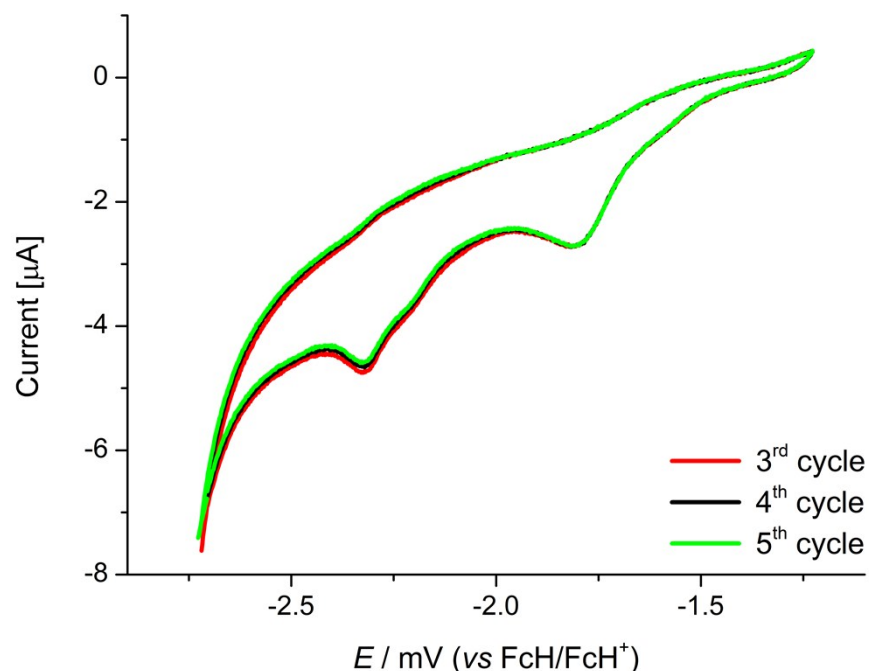


**Figure S16.** Set of cyclic voltammograms of  $\{\text{TPPFc}_8(\text{H}_2\text{O})_2\}$  in  $\text{CH}_2\text{Cl}_2$  ( $0.5 \text{ mmol}\cdot\text{L}^{-1}$ ) in the range of  $-1200$  to  $-2700$  mV (vs.  $\text{FcH}/\text{FcH}^+$ ) at  $25^\circ\text{C}$ , supporting electrolyte  $0.1 \text{ mol}\cdot\text{L}^{-1}$   $[\text{N}(\text{nBu})_4][\text{B}(\text{C}_6\text{F}_5)_4]$ , platinum working electrode. Decamethyl ferrocene was used as an internal reference.

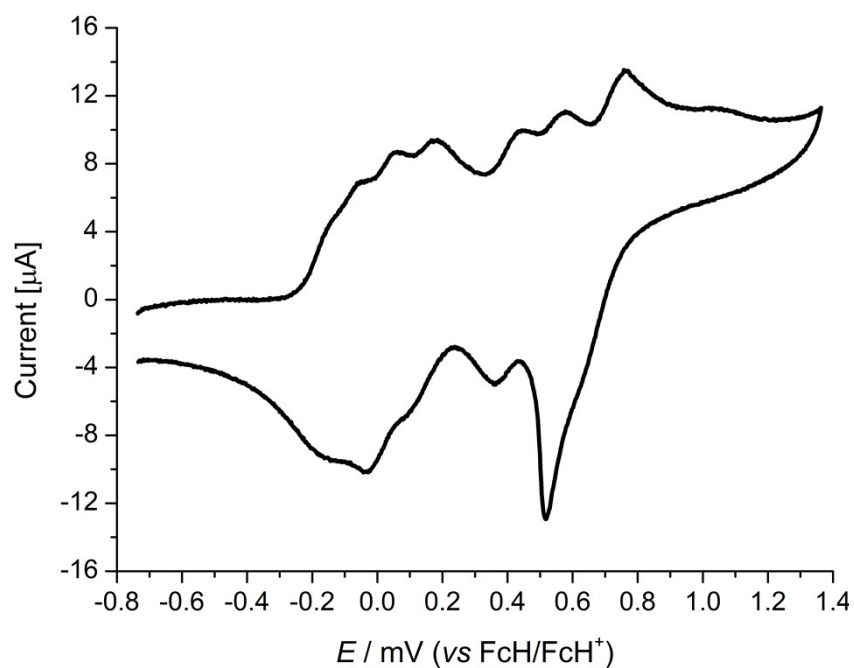


**Figure S17.** Cyclic voltammogram of  $\{\text{TPPFc}_8(\text{H}_2\text{O})_2\}$  in  $\text{CH}_2\text{Cl}_2$  ( $0.5 \text{ mmol}\cdot\text{L}^{-1}$ ) at rising potential to  $+1400$  mV (vs.  $\text{FcH}/\text{FcH}^+$ ) at  $25^\circ\text{C}$ , supporting electrolyte  $0.1 \text{ mol}\cdot\text{L}^{-1}$   $[\text{N}(\text{nBu})_4][\text{B}(\text{C}_6\text{F}_5)_4]$ , Carbon working electrode. Decamethyl ferrocene was used as an internal reference.

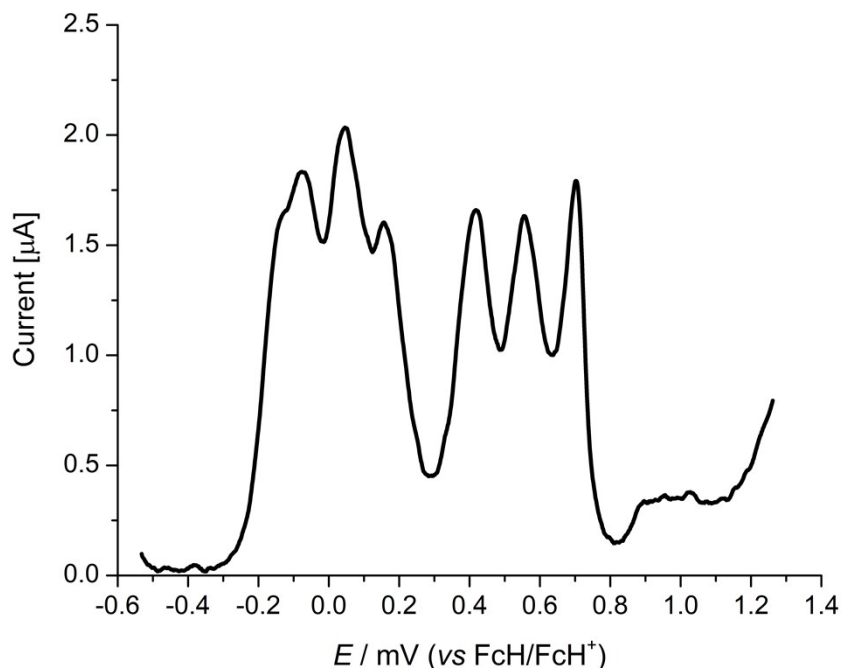


**Figure S18.** Square wave voltammogram of  $\{\text{TPPFc}_8(\text{H}_2\text{O})_2\}$  in  $\text{CH}_2\text{Cl}_2$  ( $0.5 \text{ mmol}\cdot\text{L}^{-1}$ ) at rising potential to +1400 mV (vs.  $\text{FcH}/\text{FcH}^+$ ) at 25 °C, supporting electrolyte  $0.1 \text{ mol}\cdot\text{L}^{-1}$   $[\text{N}(\text{nBu})_4][\text{B}(\text{C}_6\text{F}_5)_4]$ , Carbon working electrode. Decamethyl ferrocene was used as an internal reference. (step-height: 25 mV; pulse-width: 2 s; amplitude: 2 mV).

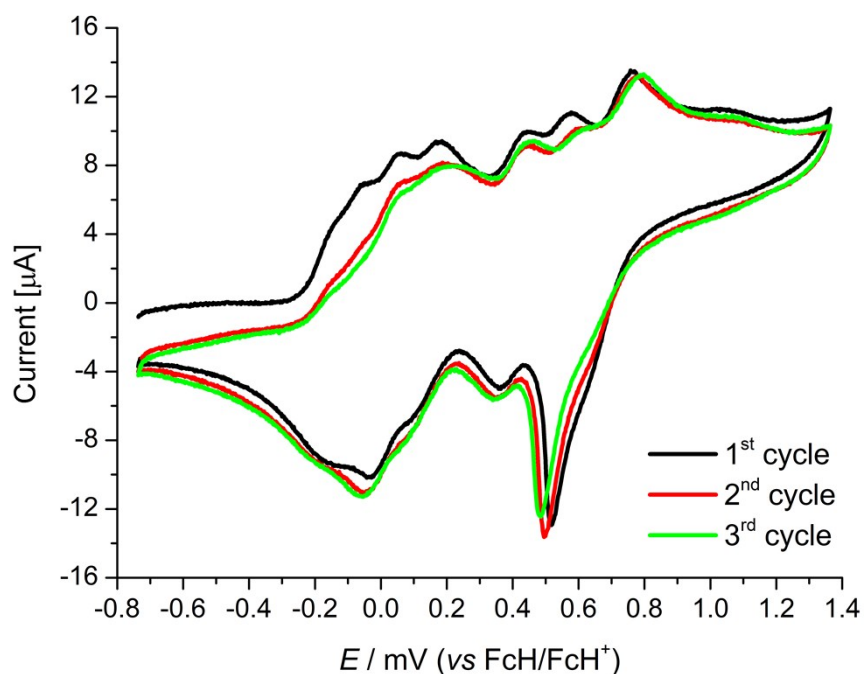
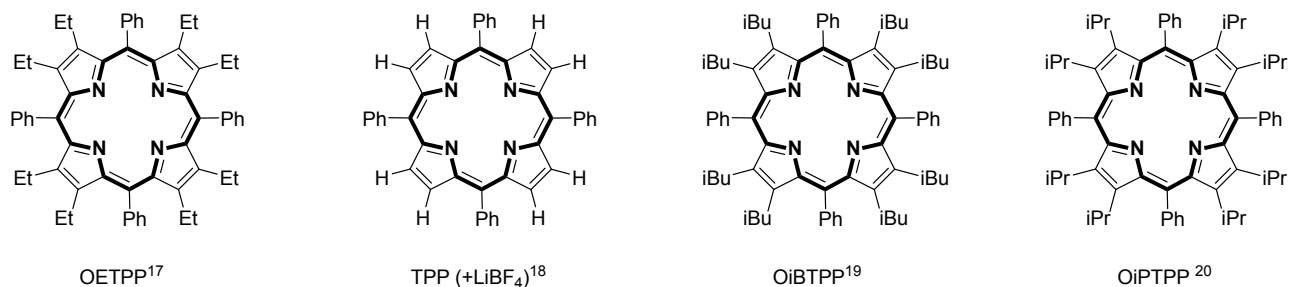


**Figure S19.** Set of cyclic voltammograms of  $\{\text{TPPFc}_8(\text{H}_2\text{O})_2\}$  in  $\text{CH}_2\text{Cl}_2$  ( $0.5 \text{ mmol}\cdot\text{L}^{-1}$ ) at rising potential to +1400 mV (vs.  $\text{FcH}/\text{FcH}^+$ ) at 25 °C, supporting electrolyte  $0.1 \text{ mol}\cdot\text{L}^{-1}$   $[\text{N}(\text{nBu})_4][\text{B}(\text{C}_6\text{F}_5)_4]$ , carbon working electrode. Decamethyl ferrocene was used as an internal reference.

#### 4. Selected antiaromatic 16 $\pi$ tetraphenylporphyrins



Compound	$\lambda_{\max}$	Log $\epsilon$
[Li(TPP)] <sup>+</sup> [BF <sub>4</sub> ] <sup>-</sup>	332 / 394	-
OETPP	275 / 339	4.52 / 4.78
OiBTTP	274/330.5	-
OiPTTP	280 / 330	4.52 / 4.76

**Scheme S3.** Chemical structures of selected antiaromatic 16 $\pi$  tetraphenylporphyrins and UV-vis data of CH<sub>2</sub>Cl<sub>2</sub> solutions of them.

#### 5. Crystallography

##### 5.1 Experimental details

All data were collected with an Rigaku Oxford Gemini S diffractometer. For data collection, cell refinement and data reduction the software CrysAlisPro was used.<sup>21</sup> All structures were solved by direct methods with SHELXS-2013 and refined by full-matrix least-squares procedures on F<sub>2</sub> using SHELXL-2013.<sup>22</sup> All non-hydrogen atoms were refined anisotropically. All C-bonded hydrogen atoms were refined by a riding model. The positions of O-bonded hydrogen atoms were taken from the difference Fourier map and refined isotropically with appropriate restraints.

Crystals of **CuTPPBr<sub>8</sub>** were obtained by slow evaporation of a dichloromethane solution which was placed in a test tube in a closed vessel containing n-hexane. The colour of the crystals appeared as green and they were all well-shaped in form of octahedrons, although their size was rather tiny (max. dimension 0.05 mm). The asymmetric unit comprises half of a dichloromethane packing solvent, which is statistically disordered along a four-fold screw-axis and which is further dynamically disordered. The occupation factor was finally adjusted to each 0.5 and a composition of **CuTPPBr<sub>8</sub>·2CH<sub>2</sub>Cl<sub>2</sub>** was revealed.

Crystals of **TPPFc<sub>8</sub>** were obtained by slow evaporation of a dichloromethane solution including a little amount of dimethylformamide (ratio CH<sub>2</sub>Cl<sub>2</sub>:DMF = 40:1 (v:v)), which was placed in a test tube in a closed vessel containing n-hexane. Upon time CH<sub>2</sub>Cl<sub>2</sub> did evaporate (partially) into the n-hexane and the mother liquor did decolour. Exclusively purple coloured and plate-like crystals were observed, which were rapidly losing their packing solvent once take from the mother liquor. Furthermore, these plate-like crystals appeared as the superposition of at least two very thin plates, which could not be separated from each other. The

dichloromethane packing solvents were refined as follows: Two of them (C1CC, C11, C12 and C4CC, C17, C18) were refined fully occupied and not disordered. Another two of them (C2CC, C13, C14 and C6CC, C111, C112) were refined fully occupied but disordered with split occupancies of 0.77/0.23 and 0.47/0.53, respectively. Another two of them (C3CC, C15, C16 and C5CC, C19, C110) were refined with an occupation factor of 0.5 and dynamic disorder with split occupancies of 0.29/0.71 and 0.24/0.76, respectively. At the final stage of the refinement the commands TWIN and BASF were used in order to refine the data as those of an inversion twin. As result a well-defined Flack  $x$  parameter of 0.454(8) was obtained. The crystallographic characterization thus revealed the composition of the single crystals as  $\{\text{TPPFc}_8(\text{H}_2\text{O})_2\} \cdot 5\text{CH}_2\text{Cl}_2$ .

## 5.2 Structural Data of $\text{CuTPPBr}_8 \cdot 2\text{CH}_2\text{Cl}_2$ and $\{\text{TPPFc}_8(\text{H}_2\text{O})_2\} \cdot 5\text{CH}_2\text{Cl}_2$

**Table S5.** Selected crystallographic and structural refinement data of  $\text{CuTPPBr}_8 \cdot 2\text{CH}_2\text{Cl}_2$  and  $\{\text{TPPFc}_8(\text{H}_2\text{O})_2\} \cdot 5\text{CH}_2\text{Cl}_2$

Compound	$\text{CuTPPBr}_8 \cdot 2\text{CH}_2\text{Cl}_2$	$\text{TPPFc}_8 \cdot 5\text{CH}_2\text{Cl}_2 \cdot 2\text{H}_2\text{O}$
Empirical Formula	$\text{C}_{46}\text{H}_{24}\text{Br}_8\text{Cl}_{14}\text{CuN}_4$	$\text{C}_{129}\text{H}_{106}\text{Cl}_{10}\text{Fe}_8\text{N}_4\text{O}_2$
Temperature (K)	116	110
Formula mass (g/mol)	1477.31	2545.47
Radiation	Cu $K\alpha$	Cu $K\alpha$
Wavelength (Å)	1.54184	1.54184
Crystal system	tetragonal	monoclinic
Space group	$I4_1/a$	$P2_1$
$a$ (Å)	20.6006(8)	15.1184(3)
$b$ (Å)	20.6006(8)	23.6167(6)
$c$ (Å)	10.1020(6)	15.6626(5)
$\alpha$ (°):	90.0	90.0
$\beta$ (°):	90.0	92.824(2)
$\gamma$ (°):	90.0	90.0
$V$ (Å <sup>3</sup> )	4287.1(4)	5585.5(3)
$Z$	4	2
$D_{\text{calc}}$ (g/cm <sup>3</sup> )	2.289	1.514
$\mu$ (mm <sup>-1</sup> )	12.099	10.719
$F(000)$	2820	2604
$\theta_{\text{min}} / \theta_{\text{max}}$ (°)	6.503/62.896	3.743 / 63.994
Reflections collected	3190	17700
Limiting indices	$-19 \leq h \leq 19$ $-23 \leq k \leq 15$ $-15 \leq l \leq 3$	$-17 \leq h \leq 10$ $-27 \leq k \leq 25$ $-18 \leq l \leq 18$
Reflections unique	1674	12508
$R_{\text{int}}$	0.0293	0.0601
Reflections observed [ $I > 2\sigma(I)$ ]	1458	10254
Data/Restraints/Parameters	1674/8/154	12508/2232/1301
$R_1 / wR_2$ [ $I > 2\sigma(I)$ ]	0.0461 / 0.1305	0.0862 / 0.2215
$R_1 / wR_2$ [all data]	0.0537 / 0.1350	0.1029 / 0.2405
Goodness-of-fit on $F^2$	1.075	0.999
Absolute structure parameter <sup>23</sup>	—	0.454(8)
Largest diff. peak/hole (eÅ <sup>-3</sup> )	0.638 / -0.797	1.346 / -0.918

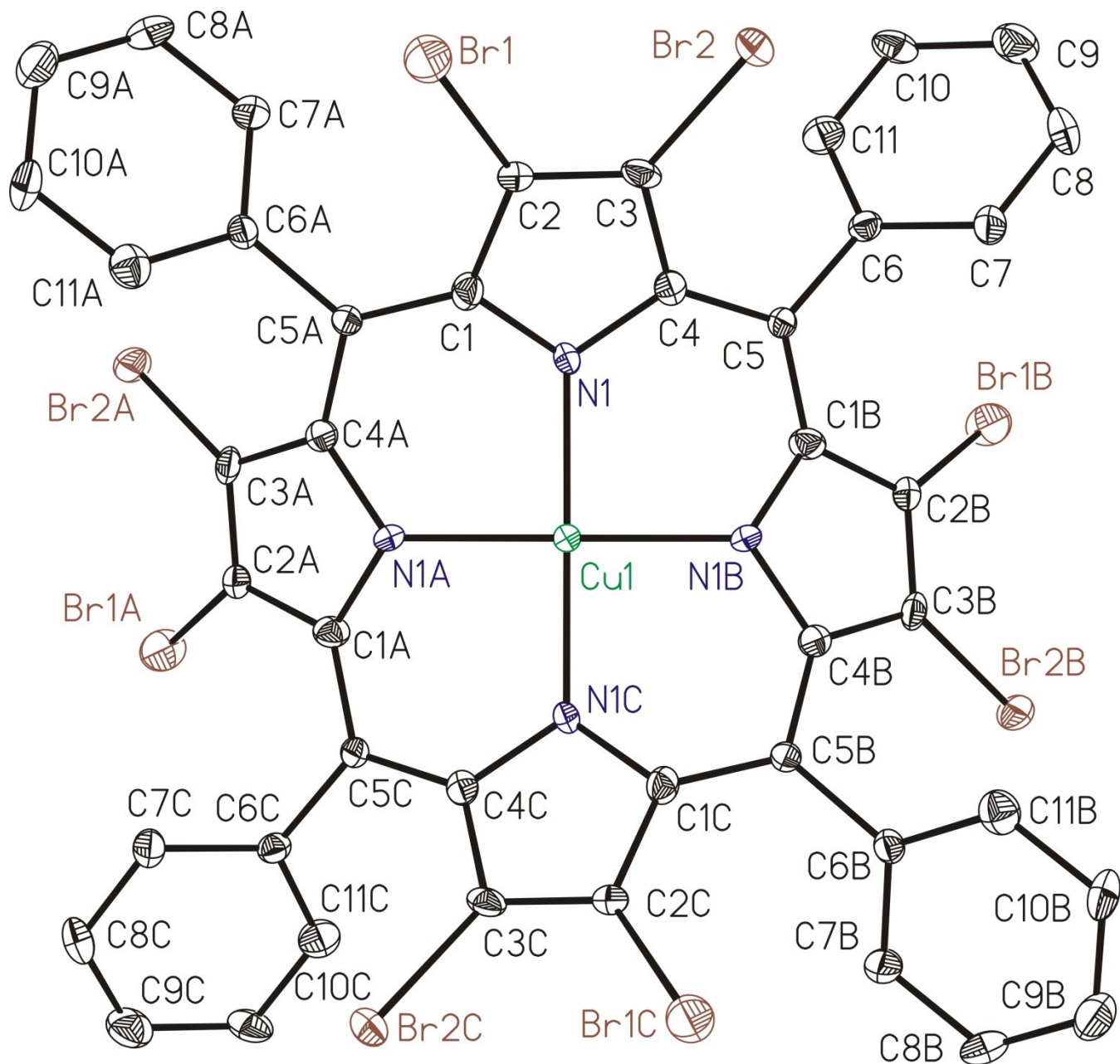


**Figure S20.** ORTEP (50 % probability ellipsoids) of the molecular structure of **CuTPPBr<sub>8</sub>·2CH<sub>2</sub>Cl<sub>2</sub>**. All hydrogen atoms and packing solvent molecules were omitted for clarity. Symmetry codes: “A” =  $-x + 1, -y + 1/2, z$ . “B” =  $-y + 3/4, x - 1/4, -z - 1/4$ . “C” =  $y + 1/4, -x + 3/4, -z - 1/4$ .



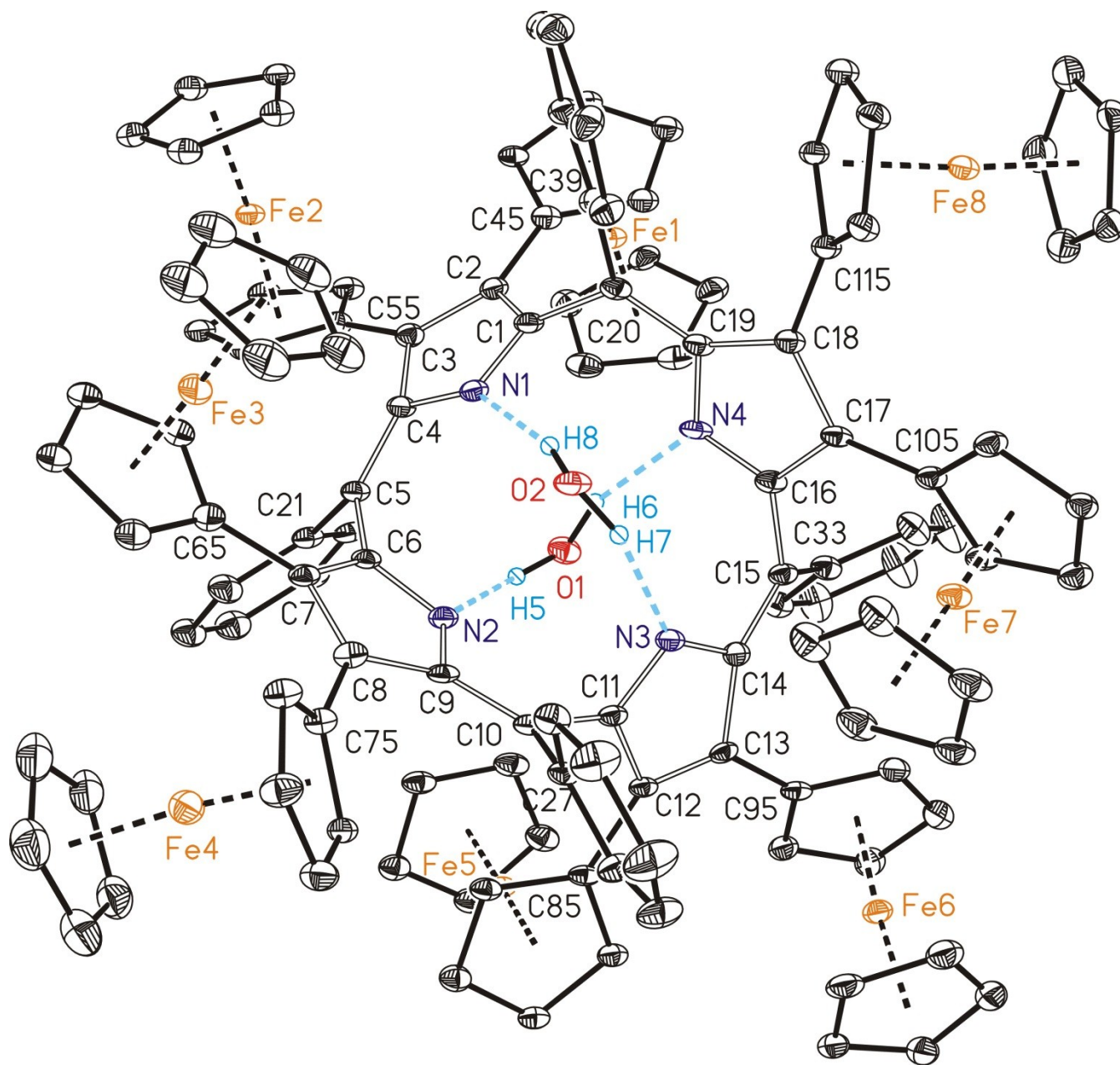


**Figure S21.** ORTEP (30 % probability ellipsoids) of the molecular structure of  $\{\text{TPPFc}_8(\text{H}_2\text{O})_2\} \cdot 5\text{CH}_2\text{Cl}_2$ . All carbon-bonded hydrogen atoms and packing solvent molecules were omitted for clarity. Of disordered atoms only one atomic position is displayed.

**Table S6.** Bond lengths (Å) and angles (°) of the hydrogen bonds of  $\{\text{TPPFc}_8(\text{H}_2\text{O})_2\} \cdot 5\text{CH}_2\text{Cl}_2$ .

D-H...A	D-H	H...A	D...A	D-H...A
O1-H5...N2	0.99(10)	2.06(9)	3.013(14)	159(9)
O1-H6...N4	1.00(9)	2.05(10)	3.014(14)	162(9)
O2-H7...N3	0.98(11)	2.03(11)	2.963(14)	158(8)
O2-H8...N1	0.95(9)	1.96(9)	2.893(14)	166(8)

**Table S7.** Selected bond lengths (Å) and angles (°) of **CuTPPBr<sub>8</sub>·2CH<sub>2</sub>Cl<sub>2</sub>** and **{TPPFc<sub>8</sub>(H<sub>2</sub>O)<sub>2</sub>}·5CH<sub>2</sub>Cl<sub>2</sub>**.

Bond lengths									
<b>CuTPPBr<sub>8</sub>·2CH<sub>2</sub>Cl<sub>2</sub></b>		<b>{TPPFc<sub>8</sub>(H<sub>2</sub>O)<sub>2</sub>}·5CH<sub>2</sub>Cl<sub>2</sub></b>							
C1–N1	1.379(8)	C1–N1	1.311(17)	C6–N2	1.327(16)	C11–N3	1.289(16)	C16–N4	1.305(16)
C1–C2	1.452(9)	C1–C2	1.471(19)	C6–C7	1.466(19)	C11–C12	1.493(17)	C16–C17	1.494(17)
C2–C3	1.355(10)	C2–C3	1.396(18)	C7–C8	1.379(18)	C12–C13	1.317(17)	C17–C18	1.436(16)
C3–C4	1.440(9)	C3–C4	1.472(18)	C8–C9	1.460(19)	C13–C14	1.488(16)	C18–C19	1.460(18)
C4–N1	1.372(8)	C4–N1	1.439(17)	C9–N2	1.395(17)	C14–N3	1.401(17)	C19–N4	1.405(16)
C4–C5	1.422(9)	C4–C5	1.349(17)	C9–C10	1.368(18)	C14–C15	1.371(18)	C19–C20	1.366(18)
C5–C1B	1.392(9)	C5–C6	1.508(18)	C10–C11	1.507(18)	C15–C16	1.481(17)	C20–C1	1.512(18)
Bond angles									
N1–C1–C5A	123.0(6)	N1–C1–C20	116.4(11)	N2–C6–C5	114.3(11)	N3–C11–C10	118.0(11)	N4–C16–C15	117.2(11)
N1–C1–C2	107.4(6)	N1–C1–C2	113.8(11)	N2–C6–C7	113.8(11)	N3–C11–C12	113.0(11)	N4–C16–C17	114.6(10)
C1–C5A–C6A	122.4(6)	C1–C20–C39	113.6(10)	C6–C5–C21	112.7(9)	C11–C10–C27	112.0(10)	C16–C15–C33	116.4(10)
C5A–C1–C2	128.7(6)	C2–C1–C20	129.6(11)	C7–C6–C5	131.9(10)	C10–C11–C12	128.8(10)	C17–C16–C15	128.2(11)
C1–C5A–C4A	120.0(6)	C1–C20–C19	118.7(11)	C4–C5–C6	120.0(12)	C9–C10–C11	117.7(11)	C16–C15–C14	117.4(12)
C4–C5–C6	117.7(6)	C4–C5–C21	126.3(11)	C9–C10–C27	129.0(12)	C14–C15–C33	124.9(11)	C19–C20–C39	126.7(11)
C1–C2–C3	108.0(6)	C1–C2–C3	105.9(11)	C6–C7–C8	104.6(10)	C11–C12–C13	105.3(10)	C16–C17–C18	102.3(10)
C1–C2–Br1	127.3(5)	C1–C2–C45	121.4(11)	C6–C7–C65	123.3(16)	C11–C12–C85	120.8(10)	C16–C17–C105	126.4(10)
C2–C3–C4	107.0(6)	C2–C3–C4	104.6(11)	C7–C8–C9	105.8(11)	C12–C13–C14	106.4(10)	C17–C18–C19	106.2(10)
C3–C2–Br1	123.8(5)	C3–C2–C45	132.7(12)	C8–C7–C65	132.1(17)	C13–C12–C85	133.9(11)	C18–C17–C105	131.1(11)
Br1–C3–C4	128.2(5)	C55–C3–C4	122.6(10)	C75–C8–C9	121.3(10)	C95–C13–C14	119.5(10)	C19–C18–C115	122.3(9)
C2–C3–Br2	124.2(5)	C2–C3–C55	132.7(11)	C7–C8–C75	132.9(11)	C12–C13–C95	134.1(10)	C17–C18–C115	131.1(11)
C3–C4–C5	128.4(6)	C3–C4–C5	132.5(12)	C8–C9–C10	131.5(13)	C13–C14–C15	133.5(12)	C18–C19–C20	130.7(12)
C1–N1–C4	108.0(5)	C1–N1–C4	104.6(10)	C6–N2–C9	104.3(11)	C11–N3–C14	105.5(10)	C16–N4–C19	106.0(10)
N1–C4–C3	108.9(6)	N1–C4–C3	110.2(10)	N2–C9–C8	110.9(10)	N3–C14–C13	108.6(10)	N4–C19–C18	110.4(10)
N1–C4–C5	122.6(6)	N1–C4–C5	115.8(11)	N2–C9–C10	117.0(12)	N3–C14–C15	116.8(10)	N4–C19–C20	117.9(12)

**Table S8.** Bond lengths (Å) and angles (°) of the CuN<sub>4</sub> coordination unit of CuTPPBr<sub>8</sub>·2CH<sub>2</sub>Cl<sub>2</sub>.

<u>Bond length</u>	<u>Bond angles<sup>a)</sup></u>	
Cu1–N1 1.968(5)	N1–Cu1–N1A	90.150(15)
	N1–Cu1–N1B	90.150(15)
	N1–Cu1–N1C	174.1(3)
	Cu1–N1–C1	121.6(4)
	Cu1–N1–C4	124.0(4)

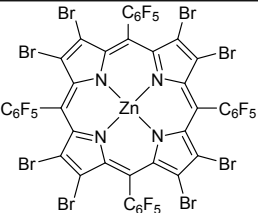
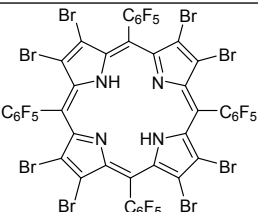
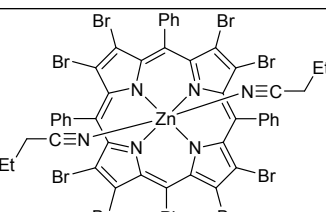
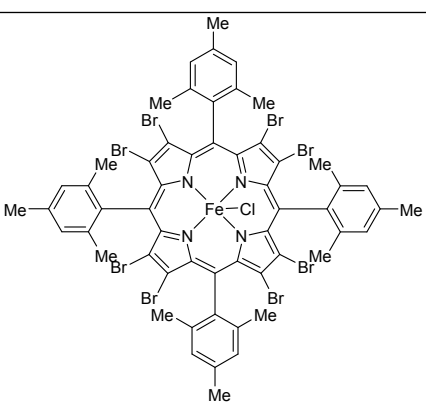
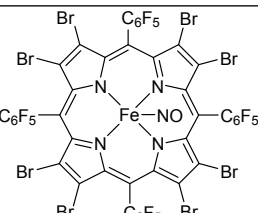
a) Symmetry codes: “A” =  $-x + 1, -y + 1/2, z$ . “B” =  $-y + 3/4, x - 1/4, -z - 1/4$ . “C” =  $y + 1/4, -x + 3/4, -z - 1/4$ .

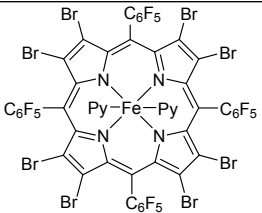
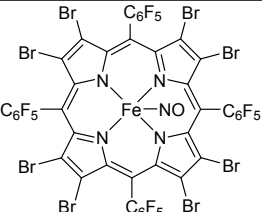
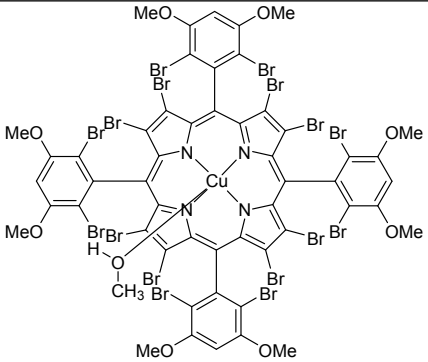
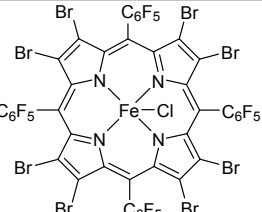
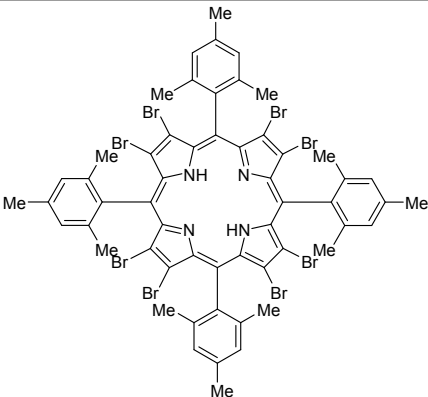
**Table S9.** Selected torsion angles (°) of **CuTPPBr<sub>8</sub>·2CH<sub>2</sub>Cl<sub>2</sub>** and **{TPPFc<sub>8</sub>(H<sub>2</sub>O)<sub>2</sub>}·5CH<sub>2</sub>Cl<sub>2</sub>**.

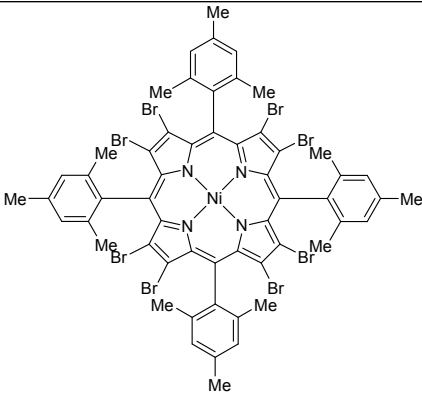
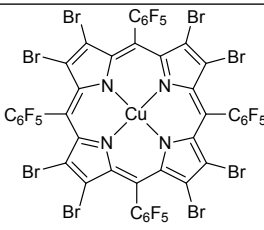
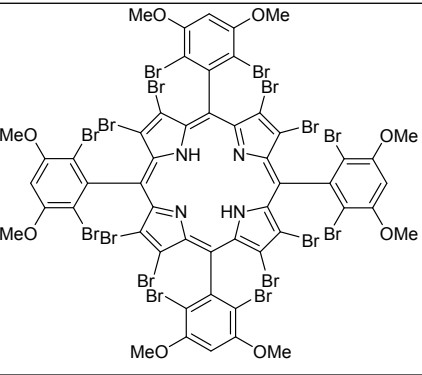
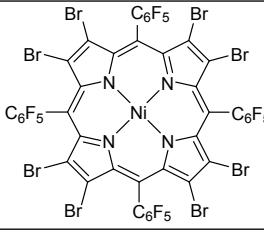
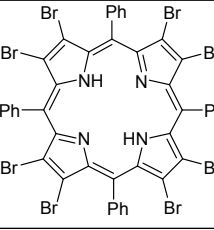
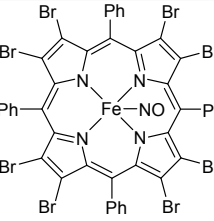
Torsion angles									
<b>CuTPPBr<sub>8</sub>·2CH<sub>2</sub>Cl<sub>2</sub></b>		<b>{TPPFc<sub>8</sub>(H<sub>2</sub>O)<sub>2</sub>}·5CH<sub>2</sub>Cl<sub>2</sub></b>							
C4–C5–C1B–N1B	-16.1(7)	C19–C20–C1–N1	79.8(15)	C4–C5–C6–N2	-86.3(14)	C9–C10–C11–N3	83.4(15)	C14–C15–C16–N4	86.3(15)
		C20–C1–N1–C4	179.8(10)	C5–C6–N2–C9	177.6(9)	C10–C11–N3–C14	178.4(10)	C15–C16–N4–C19	178.8(11)
		C1–N1–C4–C5	159.5(11)	C6–N2–C9–C10	-164.3(10)	C11–N3–C14–C15	159.9(11)	C16–N4–C19–C20	-164.5(12)
		N1–C4–C5–C6	10.7(17)	N2–C9–C10–C11	-1.6(15)	N3–C14–C15–C16	7.2(17)	N4–C19–C20–C1	0.6(18)

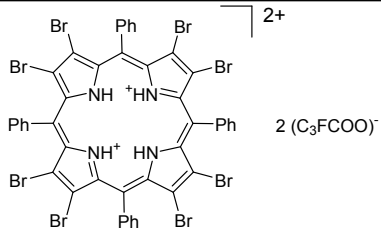
5.3  $\beta$ -2,3,7,8,12,13,17,18-Octabromo-meso-5,10,15,20-tetraphenyl(metallo) porphyrins ( $H_2TAr_4Br_8 / MTAr_4Br_8$ )

Table S10. CSD RefCodes of octabromoporphyrins together with their chemical structure and MD parameter.

CSD-RefCode	Chemical structure	MD
LALRIZ <sup>24</sup>		0.424
ZALJEB <sup>25</sup>		0.442
PESRIO <sup>26</sup>		0.464
PEXHOP <sup>27</sup>		0.490
SURGUJ <sup>28</sup>		0.495

ZEQRAO <sup>29</sup>		0.499
SURHAQ <sup>28</sup>		0.510
FEYMUS <sup>30</sup>		0.526
ZEQUUH <sup>29</sup>		0.537
PAHKEO <sup>31</sup>		0.542

PAHKIS <sup>31</sup>		0.574
LATSEE <sup>32</sup>		0.578
TIZTEC <sup>33</sup>		0.604
PAHKOY <sup>31</sup>		0.614
RONROB <sup>34</sup>		0.616
ZESHOU <sup>35</sup>		0.629

YEVKUF <sup>36</sup>		0.684
----------------------	--	-------

## 6. Computational Details

The BP86 functional<sup>37,38</sup> in combination with the TZVP basis set<sup>39</sup> was employed for structure optimization for which the ORCA<sup>40</sup> program package was used. Dispersion forces were considered by an empirical dispersion correction proposed by Grimme.<sup>41,42</sup> The structure optimization was speeded up by the split resolution of identity approximation (Split-RI-J).<sup>43-46</sup> After structure optimization, Turbomole<sup>47</sup> was employed with the same basis set and functional as in the calculations with ORCA to obtain nuclear magnetic shielding constants. The multipole accelerated resolution of identity approximation<sup>43-45,48</sup> (MARI-J) was employed to speed up the single point calculation while NMR shielding was calculated by the gauge including atomic orbital (GIAO) method.<sup>49</sup> NBO 6.0<sup>50</sup> as implemented in the Jaguar 9.3 program package<sup>51</sup> was employed to calculate the Wiberg bond index.<sup>52</sup> BP86 in combination with a 6-31G\* basis set<sup>53,54</sup> for all organic compounds and the LACVP basis set<sup>55</sup> for Fe was used to obtain the electronic structure analyzed by the NBO program.

## 7. References

- Perrin, D. D.; Armarego, W. L. F. In *Purification of Laboratory Chemicals*, Pergamon, New York, 3rd ed.; **1988**.
- Adler, A. D.; Longo, F. R.; Finarelli, J. D.; Goldmacher, J.; Assour, J.; Korsakoff, L. A. *J. Org. Chem.* **1967**, *32*, 476–476.
- Adler, A. D.; Longo, F. R.; Kampas, F.; Kim, J. *J. Inorg. Nucl. Chem.* **1970**, *32*, 2443–2445.
- Pfaff, U.; Hildebrandt, A.; Schaarschmidt, D.; Ruffer, T.; Low, P. J.; Lang, H. *Organomet.* **2013**, *32*, 6106–6117.
- LeSuer, R. J.; Buttolph, C.; Geiger, W. E. *Anal. Chem.* **2004**, *76*, 6395–401.
- Clark, H. C.; Goel, A. B. *Inorg. Chim. Acta* **1978**, *31*, L441–L442.
- Shi, B.; Boyle, R. W. *J. Chem. Soc., Perkin Trans.* **2002**, *1*, 1397–1400.
- (a) Alben J. O. in *The Porphyrins*, Dolphin, D., Eds.; Academic Press: New York, NY, USA, 1978; *2*, 323–345. (b) Feng, Y.; Chen, S.; Guo, W.; Zhang, Y.; Liu, G. *J. Electroanal. Chem.* **2007**, *602*, 115–122.
- Saphier, M.; Yifrah, T.; Zilbermann, I.; Saphier, O.; Shames, A. I.; Froumin, N.; Meyerstein, D.; Guldi, D. *J. Porphyrins Phthalocyanines* **2012**, *16*, 1124–1131.
- Wahab, A.; Bhattacharya, M.; Ghosh, S.; Samuelson, A. G.; Das, P. K. *J. Phys. Chem. B* **2008**, *112*, 2842–2847.
- Liu, C.; Chen, Q-Y. *Eur. J. Org. Chem.* **2005**, 3680–3686.



- (12) Rosenblum, M.; Woodward, R. B. *J. Am. Chem. Soc.* **1958**, *80*, 5443–5449.
- (13) Lehrich, S. W.; Hildebrandt, A.; Ruffer, T.; Korb, M.; Low, P.; Lang, H. *Organomet.* **2014**, *33*, 4836–4845.
- (14) Poppitz, E. A.; Hildebrandt, A.; Korb, M.; Schaarschmidt, D.; Lang, H. *Z. Anorg. Allg. Chem.* **2014**, *640*, 2809–2816.
- (15) Hildebrandt, A.; Lang, H. *Organomet.* **2013**, *32*, 5640–5653.
- (16) Manke, A. –M.; Geisel, K.; Fetzer, A.; Kurz, P. *Phys. Chem. Chem. Phys.* **2014**, *16*, 12029–12042.
- (17) Yamamoto, Y.; Yamamoto, A.; Furuta, S.-Y.; Horie, M.; Kodama, M.; Sato, W.; Akiba, K.-Y.; Tsuzuki, S.; Uchimar, T.; Hashizume, D.; Iwasaki, F. *J. Am. Chem. Soc.* **2005**, *127*, 14540–14541.
- (18) Kakui, T.; Sugawara, S.; Hirata, Y.; Kojima, S.; Yamamoto, Y. *Chem. Eur. J.* **2011**, *17*, 7768–7771.
- (19) Yamamoto, Y.; Hirata, Y.; Kodama, M.; Yamaguchi, T.; Matsukawa, S.; Akiba, K.-Y.; Hashizume, D.; Iwasaki, F.; Muranaka, A.; Uchiyama, M.; Chen, P.; Kadish, K. M.; Kobayashi, N. *J. Am. Chem. Soc.* **2010**, *132*, 12627–12638.
- (20) Sugawara, S.; Kodama, M.; Hirata, Y.; Kojima, S.; Yamamoto, Y. *J. Porphyrins Phthalocyanines* **2011**, *15*, 1326–1334.
- (21) CrysAlisPro, Agilent Technologies, Version 1.171.37.35 (release 13-08-2014 CrysAlis171.NET).
- (22) Sheldrick, G. M. *Acta Crystallogr., Sect. A: Fundam. Crystallogr.* **2008**, *64*, 112–122.
- (23) Flack, H. D. *Acta Crystallogr., Sect. A: Fundam. Crystallogr.* **1983**, *39*, 876.
- (24) Marsh, R. E.; Schaefer, W. P.; Hodge, J. A.; Hughes, M. E.; Gray, H. B.; Lyons, J. E.; Ellis, P. E. *Acta Cryst.* **1993**, 1339–1342.
- (25) Birnbaum, E. R.; Hodge, J. A.; Grinstaff, M. W.; Schaefer, W. P.; Henling, L.; Labinger, J. A.; Bercaw, J. E.; Gray, H. B. *Inorg. Chem.* **1995**, *34*, 3625–3632.
- (26) Bhyrappa, P.; Krishnan, V.; Nethaji, M. *J. Chem. Soc. Dalton Trans.* **1993**, 1901–1906.
- (27) Ochsenbein, P.; Mandon, D.; Fischer, J.; Weiss, R.; Austin, R. N.; Jayaraj, K.; Gold, A.; Ternner, J.; Bill, E.; Muther, M.; Trautwein, A. X. *Angew. Chem., Int. Ed.* **1993**, *32*, 1437–1439.
- (28) Hu, B.; Li, J. *Angew. Chem., Int. Ed.* **2015**, *54*, 10579–10582.
- (29) Grinstaff, M. W.; Hill, M. G.; Birnbaum, E. R.; Schaefer, W. P.; Labinger, J. A.; Gray, H. B. *Inorg. Chem.* **1995**, *34*, 4896–4902.
- (30) Bhyrappa, P.; Purushothaman, B.; Vittal, J. J. *J. Porphyrins Phthalocyanines* **2003**, *7*, 682–692.
- (31) Mandon, D.; Ochsenbein, P.; Fischer, J.; Weiss, R.; Jayaraj, K.; Austin, R. N.; Gold, A.; White, P. S.; Brigaud, O.; Battioni, P.; Mansuy, D. *Inorg. Chem.* **1992**, *31*, 2044–2049.
- (32) Henling, L. M.; Schaefer, W. P.; Hodge, J. A.; Hughes, M. E.; Gray, H. B. *Acta Cryst.* **1993**, 1743–1747.
- (33) Bhyrappa, P.; Arunkumar, C.; Varghese, B. *J. Porphyrins Phthalocyanines* **2007**, *11*, 795–804.
- (34) Spyroulias, G. A.; Despotopoulos, A.; Raptopoulou, C. P.; Terzis, A.; Coutsolelos, A. G. *Chem. Commun.* **1997**, 783–784.
- (35) Bohle, D. S.; Hung, C.-H. *J. Am. Chem. Soc.* **1995**, *117*, 9584–9585.
- (36) Senge, M. O.; Forsyth, T. P.; Nguyen, L. T.; Smith, K. M. *Angew. Chem., Int. Ed.* **1994**, *33*, 2485–2487.

- (37) Becke, A. D. *Phys. Rev. A* **1988**, *38*, 3098–3100.
- (38) Perdew, J. P. *Phys. Rev. B* **1986**, *33*, 8822–8824.
- (39) Schäfer, A.; C. Huber, C.; Ahlrichs, R. *J. Chem. Phys.* **1994**, *100*, 5829–5835.
- (40) Neese, F. *WIREs Comput. Mol. Sci.* **2012**, *2*, 73–78.
- (41) Grimme, S.; Antony, J.; Ehrlich, S.; Krieg, H. *J. Chem. Phys.* **2010**, *132*, 154101–154104.
- (42) Grimme, S.; Ehrlich, S.; Goerigk, L. *J. Comput. Chem.* **2011**, *32*, 1456–1465.
- (43) Baerends, E. J.; Ellis, D. E.; P. Ros, P. *Chem. Phys.* **1973**, *2*, 41–51.
- (44) Dunlap, B. I.; Connolly, J. W. D.; Sabin, J. R. *J. Chem. Phys.* **1979**, *71*, 3396–3402.
- (45) Eichkorn, K.; Treutler, O.; Öhm, H.; Häser, M.; Ahlrichs, R. *Chem. Phys. Lett.* **1995**, *240*, 283–289.
- (46) Neese, F.; *J. Comput. Chem.* **2003**, *24*, 1740–1747.
- (47) Ahlrichs, R.; Bär, M.; Häser, M.; Horn, H.; Kölmel, C. *Chem. Phys. Lett.* **1989**, *162*, 165–169.
- (48) Sierka, M.; A. Hogekamp, A.; Ahlrichs, R. *J. Chem. Phys.* **2003**, *118*, 9136–9148.
- (49) Schreckenbach, G.; Ziegler, T. *J. Phys. Chem.* **1995**, *99*, 606–611.
- (50) Glendening, E. D.; Badenhop, J. K.; Reed, A. E.; Carpenter, J. E.; Bohmann, J. A.; Morales, C. M.; Landis, C. R.; Weinhold, F. Nbo 6.0, University of Wisconsin, Madison, **2013**, <http://nbo6.chem.wisc.edu/>.
- (51) Jaguar; version 9.3; Schrodinger, Inc., New York, NY, **2016**.
- (52) Wiberg, K. B. *Tetrahedron* **1968**, *24*, 1083–1096.
- (53) Hehre, W. J.; Ditchfield, R.; Pople, J. A. *J. Chem. Phys.* **1972**, *56*, 2257–2261.
- (54) Francl, M. M.; Pietro, W. J.; Hehre, W. J.; Binkley, J. S.; Gordon, M. S.; DeFrees, D. J.; Pople, J. A. *J. Chem. Phys.* **1982**, *77*, 3654–3665.
- (55) Hay, P. J.; Wadt, W. R. *J. Chem. Phys.* **1985**, *82*, 299–310.